

Challenging Common Paradigms in Multi-Task Learning

Cathrin Elich^{‡,1,2,3}, Lukas Kirchdorfer^{‡,1,4},
Jan M. Köhler^{*,1}, and Lukas Schott^{*,1}

¹ Bosch Center for Artificial Intelligence

² Max Planck Institute for Intelligent Systems, Tübingen, Germany

³ Max Planck ETH Center for Learning Systems

⁴ University of Mannheim

cathrin.elich@tuebingen.mpg.de, {jan.koehler, lukas.schott}@bosch.com

[‡]Work done during an internship at Bosch. ^{*}Joint senior authors.

Abstract. While multi-task learning (MTL) has gained significant attention in recent years, its underlying mechanisms remain poorly understood. Recent methods did not yield consistent performance improvements over single task learning (STL) baselines, underscoring the importance of gaining more profound insights about challenges specific to MTL. In our study, we challenge paradigms in MTL in the context of STL: First, the impact of the choice of optimizer has only been mildly investigated in MTL. We show the pivotal role of common STL tools such as the Adam optimizer in MTL empirically in various experiments. To further investigate Adam’s effectiveness, we theoretically derive a partial loss-scale invariance under mild assumptions. Second, the notion of gradient conflicts has often been phrased as a specific problem in MTL. We delve into the role of gradient conflicts in MTL and compare it to STL. For angular gradient alignment we find no evidence that this is a unique problem in MTL. We emphasize differences in gradient magnitude as the main distinguishing factor. Lastly, we compare the transferability of features learned through MTL and STL on common image corruptions, and find light evidence that MTL can lead to superior transferability. Overall, we find surprising similarities between STL and MTL suggesting to consider methods from both fields in a broader context.

Keywords: Multi-task learning · Deep Learning · Computer Vision

1 Introduction

Multi-task learning (MTL) is gaining significance in the deep learning literature and in industry applications. Especially, tasks like autonomous driving and robotics necessitate real-time execution of neural networks while obeying constraints of limited computational resources. Consequently, there is a demand for neural networks capable of simultaneously inferring multiple tasks [19, 26].

In a seminal study, Caruana [4] highlights both advantages and challenges in MTL. On the one hand, certain tasks can exhibit a symbiotic relationship,

resulting in a mutual performance enhancement when trained together. It was further suggested that features learned in a MTL scenario rely less on incidental correlations and demonstrate improved transferability. On the other hand, conflicts between tasks can arise and decrease the performance when trained jointly, also known as *negative transfer*.

Several approaches have been suggested to mitigate the issue of negative transfer among tasks during network training. Our study focuses on two main branches in the literature: First, *gradient magnitude* methods which incorporate weights to scale task-specific losses to achieve an adequate balance between tasks. Second, *gradient alignment* methods which aim to resolve conflicts in gradient vectors that may arise between tasks within a shared network backbone.

The effectiveness of the proposed MTL methods remain uncertain in the literature. Upon comparing various studies, it becomes evident that there is no definitive approach that consistently performs well across different settings [48]. This observation has been reinforced in more recent studies where competitive performance was achieved through plain unitary scaling in combination with common regularization methods [25] or tuned task weighting [49].

The current understanding of MTL is still limited and lacks a deeper comprehension of its underlying mechanisms. To address this gap, our study aims to challenge commonly held paradigms, such as the choice of optimizer, the notion of gradient alignment, gradient magnitudes, and transferability of features.

Our **contributions** are:

- The impact of off-the-shelf optimizers has received little attention in MTL benchmarks. We evaluate the Adam [22] optimizer and demonstrate its favorable performance over SGD+momentum in various experiments.
- We provide a potential explanation for Adam’s effectiveness in MTL by theoretically demonstrating a partial invariance w.r.t. to different loss scalings. Similarly, we derive a full invariance for an optimal variation of the well-established used method of uncertainty weighting [21].
- So far *gradient alignment* conflicts have mostly been considered between different tasks [7, 20, 31, 55]. We present empirical evidence that conflicts arising from gradient alignment between tasks are not exclusive and can even be more pronounced between different samples within a task.
- Corroborating the methods proposed to balance *gradient magnitude* conflicts in MTL [21, 32, 34, 49], we confirm that gradient magnitudes pose a challenge between tasks and is less pronounced between samples within a task.
- We examine the presumption of increased robustness on corrupted data as a result of MTL [24, 37]. We find light evidence that an increased number of tasks can lead to an improved transferability.

Overall, we provide a vast set of experiments and theoretical insights which challenge common paradigms and contribute to a more comprehensive understanding of MTL in computer vision to guide future research.

2 Related Work

Work in multi-task learning (MTL) can be roughly divided into three fields:

Network architectures focus on the question of how features should be shared across tasks [34, 36, 38, 50]. *Multi-task optimization (MTO)* aims to resolve imbalances and conflicts of tasks during MTL. *Task affinities* examine a grouping of tasks that should be learned together to benefit from the joint training [12, 47]. A general overview of recent works in MTL can be found in [43, 48]. Our work focuses on MTO, which we review more thoroughly in the following.

Gradient magnitude methods prevent the dominance of individual tasks by balancing them with task-specific weights. One line of works are loss-weighting methods. Here, weights are determined before any (task-wise) gradient computation and are used for a weighted aggregation of the tasks' losses. These methods consider either the task uncertainty (UW) [21], rate of change of the losses (DWA, FAMO) [30, 34], the tasks' difficulty (DTP) [14], validation performance by applying meta-learning (MOML, Auto- λ) [33, 52], or randomly chosen task weights (RLW) [28]. In line with these, the geometric mean of task losses has been used to handle the different convergence rates of the tasks [8]. An advantage of these methods is their computational efficiency as the gradient needs to be computed only once for the aggregated loss. Alternatively, other methods consider the task-specific gradients directly, e.g., by normalizing them (Grad-Norm) [6] or propose a hybrid balancing between task-wise loss and gradient scaling (IMTL, DB-MTL) [27, 32]. Furthermore, there are several adaptations for the multiple-gradient descent algorithm (MGDA) [10], e.g. for applying it efficiently in deep learning setups [44] or by introducing a stochastic gradient correction [11]. Recently, task-wise gradient weights have been estimated by treating MTL as a bargaining problem (Nash-MTL) [40], or considering a stability criterion (Aligned-MTL) [45]. Crucially, in the context of this study, all gradient magnitude methods consider *scalar* weightings of task-wise gradients within the backbone and/or heads. They do not modify the alignment of task-specific gradient vectors.

Gradient alignment methods perform more profound vector manipulations on the task-wise gradients w.r.t. to the network weights of a shared backbone before aggregating them. The underlying assumption indicates conflicting gradients as a major problem in MTL. To address this, GradDrop [7] randomly drops gradient components in the case of opposing signs. PCGrad [55] proposes to circumvent problems of conflicting gradients by projecting them onto each other's normal plane. Following this idea, Liu et al. [31] propose CAGrad to converge to a minimum of the average loss instead of any point on the Pareto front. RotoGrad [20] rotates gradients at the intersection of the heads and backbone to improve their alignment. Shi et al. [46] propose to alter the network architecture based on the occurrence of layer-wise gradient conflicts. Lastly, [41] use separate optimizers such as SGD and SGD+momentum per task. This is extended to AdaGrad, RMSProp and Adam in AdaTask [51].

Recent studies *question the effectiveness of optimization-based methods* in MTL. Xin et al. [49] execute an extensive hyperparameter search to show

that simple scalar task-weighting performs equivalent or superior to many aforementioned multi-task optimization methods. Their hyperparameter search not only include the task-weights, but also common deep learning parameters such as the learning rate and regularization. Concurrently, Kurin et al. [25] empirically show that fixed task-weights combined with regularization and stabilization techniques yield to equivalent performance compared to sophisticated multi-task optimization methods. Following these, Royer et al. [42] examine the role of model capacity for MTL performance as well as the occurrences of gradient conflicts. We extend these critical studies. In particular, we theoretically and empirically demonstrate that the choice of optimizer is crucial and could potentially help to explain discrepancies found in prior studies (4.1). We further specifically distinguish between gradient conflicts between tasks and samples (4.2).

3 Problem Statement

Multi-task learning addresses the problem of learning a set of T tasks simultaneously. We consider a supervised learning setup, use a shared backbone architecture, and learn all tasks together. Formally, given input data \mathcal{X} , the goal is to learn a function $f_{\theta}(x)$ which maps a point $\mathbf{x} \in \mathcal{X}$ to each task label y_t with $t = 1, \dots, T$. The trainable parameters $\theta = \{\phi, \psi_{1:T}\}$ consist of *shared* parameters ϕ and *task-specific* parameters ψ_t . Training a task t is associated with the loss $\mathcal{L}_t(f_{\theta}(x); \theta)$, e.g., a regression or classification loss. We denote respective gradients on the shared and task-specific parameters with $\mathbf{g}_t^{\phi} = \nabla_{\phi} \mathcal{L}_t$, and $\mathbf{g}_t^{\psi} = \nabla_{\psi} \mathcal{L}_t$. When training on multiple tasks, the shared parameters ϕ needs to be updated w.r.t. all task-wise gradients \mathbf{g}_t^{ϕ} which requires an appropriate aggregation. A simple solution is to uniformly sum up the task losses $\mathcal{L} = \sum_t \mathcal{L}_t$ which is referred to as *Equal Weighting* (EW). However, as tasks might be competing against each other, this can result in negative transfer and thus sub-optimal solutions. One way to deal with this difficulty is to adapt the *magnitude* of task-specific gradients. This can be achieved by weighting tasks during training, e.g., by scaling different losses $\mathcal{L} = \sum_t \alpha_t \mathcal{L}_t$, where $\alpha_t \geq 1$. Note that the α_t can change during training. Furthermore, the weighing can also be performed on gradient level to distinguish between shared and task-specific gradients. We refer to those approaches as *gradient magnitude* methods. Interestingly, the relationship between loss weights, network-updates and learning rate also depends on the optimizer. We show a derivation for SGD and Adam in Appendix A1.2. Additionally to adapting the gradient magnitude, one can directly adapt the *alignment* of task-wise gradient vectors within the shared backbone $\tilde{\mathbf{g}}^{\phi} = \mathbf{h}(\mathbf{g}_1^{\phi}, \dots, \mathbf{g}_T^{\phi})$.

In practice, an optimum for θ that yields best performance on all tasks often does not exist. Instead, improving performance on some task often yields a performance decrease in another task. To still enable a comparison across network instances in MTL, an instance θ^* is called to be *Pareto optimal*, if there is no other θ' such that $\mathcal{L}_t(\theta') \leq \mathcal{L}_t(\theta^*) \forall t$ with strict inequality in at least one task. The *Pareto front* consists of the Pareto optimal solutions.

4 Experiments and results

In this section, we perform several experiments to gain a more profound understanding of multi-task learning (MTL) in computer vision by questioning common paradigms. We compare the impact of Adam and SGD in MTL in Sec. 4.1, examine the process of gradient similarity in different settings in Sec. 4.2, and evaluate the generalization performance on corrupted data in Sec. 4.3. Throughout this evaluation, we repeatedly make use of common setups, which we will specify as follows and in more detail in Appendix A3.

Datasets: For our experiments, we consider three different datasets that are commonly used for evaluating MTL in computer vision: *CityScapes* [9] contains images of urban street scenes. In line with previous work, we consider the tasks of semantic segmentation (7 classes) and depth estimation. *NYUv2* [39] is an indoor dataset for scene understanding which was recorded over 464 different scenes across three different cities. Besides semantic segmentation (13-class) and depth estimation, it also contains the task of surface normal prediction. *CelebA* [35] consists of 200K face images which are labeled with 40 binary attributes.

Networks: We use network architectures with hard-parameter sharing which consist of a shared backbone and task-specific heads. For the dense prediction tasks on CityScapes and NYUv2, we compare SegNet [1] and DeepLabV3+ [5]. Experiments on CelebA are performed on a ResNet-18 [15] with an additional single linear layer for each head.

Training: For each method, we follow the loss or gradient aggregation as described in the related work, e.g., for equal weighting all task-specific losses are simply summed up to compute the joint network gradients. The learning rate is tuned separately for each approach. We use the validation set performance of the Δ_m metric as early stopping criteria. The Δ_m metric [36] measures the average relative task performance drop of a method m compared to the single-task baseline b using the same backbone and is computed as $\Delta_m = \frac{1}{T} \sum_{t=1}^T (-1)^{l_t} (M_{m,t} - M_{b,t}) / M_{b,t}$ where $l_t = 1$ if a higher value means better for measure $M_{.,t}$ of some task metric t , and 0 otherwise.

4.1 Effectiveness of Adam in multi-task learning

Challenged paradigm: The impact of the choice of standard optimizer is often disregarded and varies across studies (see Tab. A1 for an overview) when comparing MTL methods. For instance, Adam [22] was successfully used to show that random/constant weighting of tasks' losses performs competitive compared to MTO methods [25, 28, 49]. In contrast, many methods proposing adaptive, task-specific weighing methods [21, 32] use stochastic gradient descent with momentum (SGD+mom). In recent works, the optimizer choice converged to Adam and a fixed learning rate schedule [31, 34, 45, 55] without a comparison to SGD+mom.

In this part of our study, we investigate the impact of Adam and SGD+mom in conjunction with common MTO methods. We identify the choice of optimizer as a crucial confounder in the experimental setup. Compared to SGD+mom, we find that the Adam optimizer itself is a quite effective baseline in MTL and

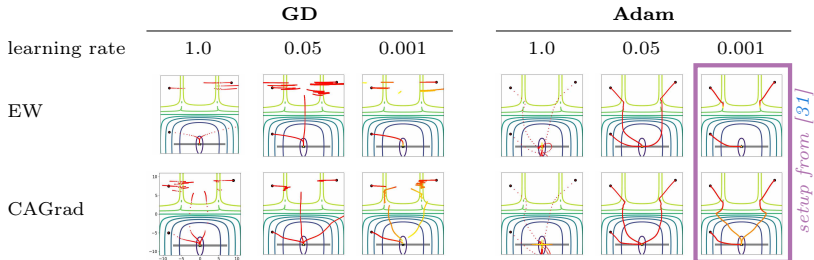


Fig. 1: Toy task experiment from CAGrad [31] for different learning rates and optimizers. Consistent with results from [49], we observe that the choice of the learning rate is crucial even for this toy optimization problem. Moreover, it becomes apparent, that selecting Adam over simple gradient decent (GD) yields superior results. The contour lines depict the 2D loss landscape; the optimization trajectories are colored from red to yellow for 100k iteration steps from three different starting points (seeds).

Table 1: Maximum number of iterations after which all seeds in the toy task experiment from CAGrad [31] reach the global minimum for varying MTO method, learning rate, and optimizer combination. In several setups, EW+Adam shows the fastest convergence to the global minimum. If not all seeds converged to the global minimum within 100k iteration steps, we denote it as $\text{?}^{\text{?}}$. As reported in previous work, we found that PCGrad converges only to some point on the Pareto Front. The **best** run for each learning rate over all MTO methods is indicated via font type.

	method	learning rate						method	learning rate				
		10.0	1.0	0.1	0.01	0.001*			10.0	1.0	0.1	0.01	0.001*
GD	EW	-	-	-	-	-	Adam	EW	26	22	709	9,015	-
	PCGrad	-	-	-	-	-		PCGrad	25	56	34,175	-	-
	CAGrad	644	213	8,069	20,418	-		CAGrad	27	32	802	11,239	57,700

to our surprise can be regarded as a loss weighting method from a theoretical viewpoint.

Toy Task Experiment To get a first impression of the impact of the optimizer and common hyperparameters such as the learning rate, we investigate the impact of Adam and plain gradient descent (GD) in a simple toy task.

Approach: We repeat the experiment of Liu et al. [31] using their original implementation but further test different learning rates and optimizers. They motivate their gradient alignment method CAGrad with a simple toy optimization problem in which their method reliably converges to the minimum of the average loss, while other MTO approaches would either get stuck (e.g., EW) or only convert to any point on the Pareto front (e.g., PCGrad [55], MGDA [44]).

Result: For higher learning rates with Adam optimizer, even the simple equal weighting (EW) method reaches the global optimum (cf. Fig. 1, e.g., EW+Adam, lr=0.05) and often converges even faster than dedicated MTO methods such as CAGrad (Tab. 1). Note, original results were shown for learning rate 0.001 using

Table 2: Number of Pareto optimal (PO) experiments using either Adam or SGD+momentum as optimizer. Models trained with Adam are consistently more often on the Pareto front compared to those trained with SGD+mom. The number of Adam-based runs that are not dominated by any SGD-based run (PO w.r.t. SGD) is even higher, which does not hold the other way around.

		Adam		SGD+mom.	
		PO (full)	PO w.r.t. SGD	PO (full)	PO w.r.t. Adam
CityScapes	SegNet	5	24	0	0
CityScapes	DeepLabV3	10	24	0	0
NYUv2	SegNet	11	21	1	1
NYUv2	DeepLabV3	16	21	6	6

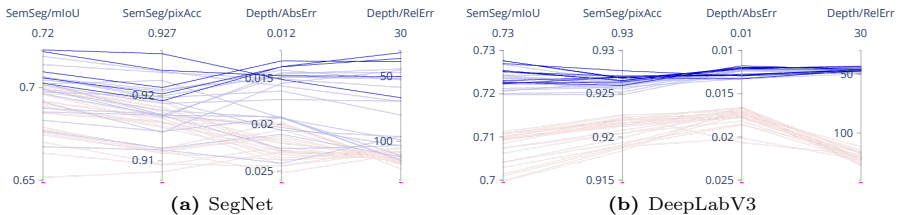


Fig. 2: Parallel coordinate plot over all experiments on CityScapes. We distinguish between experiments using **SGD+mom** and **Adam** optimizer. Experiments that reached Pareto front performance are drawn with higher saturation. We observe that Adam clearly outperforms the usage of SGD+mom.

Adam (violett outline) and were, therefore, in favor of CAGrad. Results for additional learning rates are reported in Tab. A7 and Fig. A5.

Conclusion: In summary, the choice of optimizer appears to be more important on the success of the outcome of the experiments than the choice of MTO method, as Adam converges considerably faster and more reliably than GD.

Experiments on CityScapes and NYUv2 We further extensively test the effectiveness of Adam and its role as a confounder in common MTL datasets for various MTO methods.

Approach: We compare Adam and SGD+mom in combination with any MTO method from equal weighting (EW), uncertainty weighting (UW) [21], random loss weighting (RLW) [28], PCGrad [55], CAGrad [31], IMTL [32] and Aligned-MTL [45], for which we used the implementation from [29], as well as MTL-IO [41] and AdaTask [51]. We distinguish between any combination of dataset {CityScapes [9], NYUv2 [39]} and network architecture {SegNet [1], DeepLabv3 [5]}. We run experiments for ten different initial learning rates from [0.5, 0.1, 0.05, ..., 0.00001] and select the best one w.r.t. to the validation performance. More details are described in Appendix A3.2. As different models and parameter setups can show preference towards different tasks and metrics, we are interested in those models which are Pareto optimal (PO).

Results: We observe over all experimental setups that Adam performs favorably over SGD+mom (Tab. 2). This especially holds true for experiments on CityScapes where the Pareto front for both network architectures only consists of Adam-based models. Moreover, an even larger number of Adam-based models is not dominated by any model trained with SGD+mom (PO w.r.t. SGD). For NYUv2, Adam still performs stronger but SGD+mom. also occasionally delivers a PO result. For the individual metrics, the predominance of Adam is further visualized in a parallel coordinate plot in Figs. 2 and A4. Bold lines indicate the overall Pareto optimal experiments (PO full).

In Appendix A4, we further report best Δ_m results for common MTO methods in combination with Adam or SGD+mom (Tabs. A3 to A6). Again, Adam boosts the overall performance across methods. Furthermore, when comparing the ranking of MTO methods w.r.t. the Δ_m metric, we see that the order can change based on the choice of optimizer, e.g., for Cityscapes with SegNet the best method with Adam is UW but with SGD+mom it is CAGrad. This underlines the importance of the choice of optimizer as a confounder in the experimental setup. Noteworthy, EW with Adam yields Pareto optimal results in three of the four setups (cf. Tab. A2) and is not dominated by any specialized MTO method trained in combination with SGD+mom for all dataset and network combinations. This supports claims questioning the effectiveness of specific MTO methods [25, 49]. Nonetheless, looking at the Δ_m -metric and individual metric, we see that sometimes with a small relative performance drop on one metric, significant gains on another metric can be achieved (e.g., Cityscapes+sem.sem. and depth for UW vs EW).

Conclusion: Not only a well-tuned learning rate but also the optimizer is crucial for MTL performance. In a fair and extensive experimental comparison, we were able to show that Adam shows superior performance in MTL setup compared to SGD+mom.

The reasonable effectiveness of Adam in the context of uncertainty weighting We show that Adam’s mechanism to estimate a parameter-specific learning rate is partially loss-scale invariant which could contribute to Adam’s effectiveness in MTL. We demonstrate this partial invariance theoretically and empirically. Furthermore, a full loss-scale invariance can also be shown under mild assumptions for UW [21], which is among the most prevalent loss weighting method in the literature, and related similar variant [27].

The loss-scale invariance of UW can be shown by assuming an optimal solution for the σ values similar to [23]. This assumption is mild as this is a 1-dimensional convex optimization problem for each σ . The invariance can be demonstrated by inserting the analytical solution starting from UW. For example, assuming a Laplacian distribution for simplicity (this can be shown for other distributions as well), we have

$$\min_{\sigma_t} \frac{1}{\sigma_t} \mathcal{L}_t + \log \sigma_t \Rightarrow \sigma_t = \mathcal{L}_t \quad (1)$$

The left hand side shows the typical form of UW, as shown for a Gaussian in [21, eq.(5)]. Here, \mathcal{L}_t is a task-specific loss and σ_t is a scalar parameter that is usually learned. Plugging back the optimal solution for σ_t , we get

$$\mathcal{L} = \sum_t \frac{\mathcal{L}_t}{sg[\mathcal{L}_t]} + c, \quad (2)$$

where sg is the stop-gradient operator and c is a constant that can be omitted during optimization. Given this equation, we directly see the invariance w.r.t. loss-scalings. For instance, with $\mathcal{L}_1 \rightarrow \alpha_1 \mathcal{L}_1$ and $\mathcal{L}_2 \rightarrow \alpha_2 \mathcal{L}_2$, the derivative of the total loss \mathcal{L} remains unchanged. As this invariance is shown on the loss-level, it holds for all gradient updates w.r.t. the head and backbone. Intuitively, this can explain why UW performs strongly in the context of various loss scalings such as measuring depth in centimeters, meters or inches. For further details, we refer to Appendix A1.

Similarly, for Adam, we can prove a partial scale invariance of losses in MTL that holds for the parameters of network heads. As before, we assume a hydraulic-like network architecture with a shared backbone and task-specific heads. We start with the parameter-update rule from Adam and scale the corresponding losses $\mathcal{L}_t \rightarrow \alpha_t \mathcal{L}_t$. When only considering the parameters of the corresponding heads ψ_t , the scalings α_t cancel out

$$\psi_{t,i} = \psi_{t,i-1} - \frac{\gamma}{\sqrt{\alpha_t^2 \hat{v}_t}} \alpha_t \hat{m}'_t. \quad (3)$$

Thus, for the network heads, we see a similar effect as for optimal UW that different scalings do not impact the network update. However, this does not hold for the backbone. The full derivation is shown in Appendix A1. We confirm empirically in a handcrafted loss-scaling experiment in Appendix A2 and Figs. A1 and A2 that SGD does not offer any scaling invariance, whereas Adam involves the invariance property for the heads. The optimal UW demonstrates a scaling invariance for the heads and the backbone.

We would like to note that our derivation for Adam is only valid for constant α_t , e.g., measuring depth in different units or unitary weightings [25, 49]. In case of dynamic loss weights that are not constant (e.g., UW), the weights do not cancel out fully due to the accumulation of gradient histories within Adam. Nonetheless, this has profound implications for loss weighting methods that are used in conjunction with Adam. For instance, when turning off the history within Adam (by setting $\beta_{1,2} = 0$) and having a fixed backbone, all loss weighting methods, such as UW, random loss weighting and others, become equivalent to equal weighting.

Additional ablations to our previous experiments confirm the relevance of invariance in MTL (cf. Tabs. A3 to A6). First, we compare to signSGD+mom [3] which only updates on the sign of gradients and is therefore trivially scale-invariant in the heads. In a direct comparison with SGD+mom, we observe a superiority of signSGD for a majority of tested setups. Next, we applied task-specific Adam optimizers as in AdaTask [51] for a full loss-scale invariance and to allow an estimate of task-specific momentum and squared gradient accumu-

lation. This is Pareto dominant over plain Adam+EW in almost all cases and significantly improves the Δ_m metric.

Conclusion: During MTL network training, we derive and measure a full loss-scale invariance for an optimal UW and a partial invariance for Adam. This partial invariance does not hold for SGD+mom and could explain, among other properties, the effectiveness of Adam in MTL as a baseline and its symbiotic behavior combination with other MTO methods. Thus, when comparing different loss weighting methods, it is crucial to be aware of the influence of the optimizer.

4.2 Investigating gradient conflicts between tasks and samples

Challenged paradigm: The field of MTL strongly focuses on resolving conflicts between tasks, especially from a perspective of gradient conflicts [20, 31, 55]. In computer vision, tasks are often defined on a conceptual level such as segmentation and depth (CityScapes), or recognizing multiple attributes (CelebA). However, in principle, conflicts can not only occur between tasks but also between samples within a task.

We argue that in an extreme case, even recognizing a single cat in multiple images could be considered MTL. For instance, in one image, the cat could be hiding behind a plant and only revealing its eyes, requiring a neural network to recognize the cat solely based on the eyes. In other images, the cat might only reveal its paws, front of a bright window, or might be tired and curled up into a furry ball because we took so many pictures. This would require a paw, shape or fur classifier. Thus, a neural network is required to solve multiple sub-tasks to reliably recognize our cat.



Fig. 3: High intra-task diversity can mimic MTL.

Motivated by this example, we would like to quantify inter-task and inter-sample conflicts in common datasets from a perspective of the MTO literature, which inspects gradient conflicts in neural networks. In particular, we challenge the sole focus on inter-task gradients conflicts in MTL. While several works follow the idea of overcoming gradient conflicts in MTL [20, 31, 46], their appearance has only been mildly investigated so far.

Prerequisite: We compare gradients w.r.t. network weights for different tasks t and samples \mathbf{x}_i . The alignment of two gradients \mathbf{g}, \mathbf{g}' on the shared parameters, e.g., of task a and task b , is compared with the cosine similarity

$$S_{cos}(\mathbf{g}, \mathbf{g}') = \cos(\phi) = \frac{\mathbf{g} \cdot \mathbf{g}'}{\|\mathbf{g}\| \|\mathbf{g}'\|}. \quad (4)$$

Thus, two gradients are in conflict, if their cosine similarity is smaller than zero [55]. In particular, S_{cos} is $1/-1$ if gradients point in the same/opposite direction and 0 in case of orthogonal directions. The gradient magnitude similarity

$$S_{mag}(\mathbf{g}, \mathbf{g}') = \frac{2\|\mathbf{g}\|_2 \cdot \|\mathbf{g}'\|_2}{\|\mathbf{g}\|_2^2 + \|\mathbf{g}'\|_2^2} \quad (5)$$

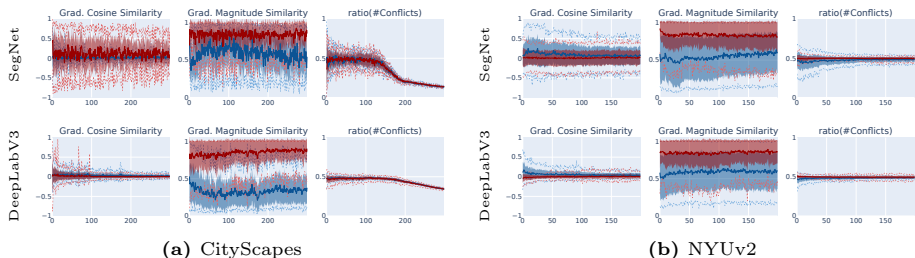


Fig. 4: Gradient similarities and conflicts for different datasets and network architectures over training epochs. For each dataset and network combination, we report (from left to right) gradient cosine similarity, gradient magnitude similarity, and the ratio of conflicting gradient parameters w.r.t. gradient pairs corresponding to either **inter-samples** (fixed task) or **inter-tasks** (fixed sample). We report mean (solid line), standard deviation (shaded area), upper (97.5%) and lower (2.5%) percentile (dotted line) within an epoch. Overall, the direction conflicts are similar (first / last column), whereas the magnitude differences are more pronounced in MTL (middle column).

as defined in [55], yields values close to 1 for gradients of similar magnitude, or close to 0 for large discrepancies in magnitude. High dissimilarity in both gradient direction and magnitude is presumed to be a common MTL problem.

Approach: During the training on aforementioned datasets, we examine gradient similarity across two different setups: (1) between gradients of different tasks with respect to a single sample (**inter-task**), e.g., $\mathbf{g} = \nabla_{\phi} L_0(f_{\theta}(\mathbf{x}_i))$ and $\mathbf{g}' = \nabla_{\phi} L_1(f_{\theta}(\mathbf{x}_i))$; and (2) between gradients corresponding to the same task but different samples within a batch (**inter-sample**), e.g., $\mathbf{g} = \nabla_{\phi} L_t(f_{\theta}(\mathbf{x}_0))$ and $\mathbf{g}' = \nabla_{\phi} L_t(f_{\theta}(\mathbf{x}_1))$. For both setups, we compute the gradient cosine similarity and gradient magnitude similarity as well as the ratio of conflicting gradient parameters. We are aware that our comparison between samples and tasks is not direct. Nonetheless, it serves as a coarse indicator to estimate their impact during network training. Implementation details are in Appendix A3.

Results: We show the evolution of the gradient similarity measures over epochs in Fig. 4. Surprisingly, when comparing inter-sample (red line) and inter-task (blue line), we find no consistent evidence for gradient alignment conflicts (left column) to be an exclusive problem of having multiple tasks. For instance, for Cityscapes, the variation of gradient alignment is fully encapsulated within the spread we observe in inter-sample variation (task is fixed). For CelebA (Fig. A6), the converse seems to be mostly the case. Furthermore, the choice of network architecture and distribution of task-specific and shared parameters (SegNet vs. DeepLabV3) can have a large influence on the spread of the cosine-similarity. Both architectures have roughly a similar number of shared-parameters. However, DeepLabV3 has a higher number of task-specific parameters which seems to reduce the variance in conflicts for both inter-sample and inter-task (row one vs. two). In line with these observations, we found a similar number of conflicting gradient parameters (third column) for both inter-sample and inter-task comparisons among all experiments.

For gradient magnitude similarities (middle column), we observe a clearer pattern. The similarity in magnitudes are continuously (in the mean) less pronounced for the inter-task setup compared to inter-samples (blue line is below red one in all settings). Interestingly, the relative difference between the two setups remains similar over training which justifies the choice of fixed scalar task weightings as done in [49]. Further measures can be found in Figures A7 to A11.

Conclusion: We find that the difficulty of MTL (inter-task and inter-sample) as opposed to STL (inter-sample only) is predominantly due to differences in gradient *magnitudes*. Although the problem of conflicting gradients has been typically associated with task-specific conflicts [20,31,55], we found that gradient *alignment* conflicts can actually be even more pronounced between samples. On the one hand, these observations are along the same lines as findings by Royer et al. [42] who reason that ‘correcting conflicting gradients [between tasks] at every training iteration can be superfluous’. On the other hand, gradient-alignment methods in MTL could be considered not only in the context of task-specific conflicts but also for conflicts between samples.

4.3 Robustness of multi-task representations on corrupted data

In the last part of our analysis, we investigate whether features learned for multiple tasks generalize better to corrupted data compared to those learned for single tasks only.

Motivation: In his seminal paper, Caruana gives preliminary evidence that MTL provides stronger features and avoids spurious correlations (referred to better *attribute selection*) [4]. More recently, spurious correlations have often been directly connected with robustness [13,18]. Results from current literature on the robustness of MTL features are mixed. While MTL is stated to increase the adversarial- and noise-robustness over STL [24,37,53], others argue features selected by MTL could be more likely to be non-causal and, therefore, less robust [2,17]. Here, we further challenge the paradigm whether MTL features lead to better robustness. We would like to nuance that we do not consider the transferability of representations, e.g., to new tasks, but solely focus on the claim that the MTL trained features are more robust w.r.t. different inputs.

Approach: In our experiment, we treat the common corruptions [16] as downstream task and compare the performance after fine-tuning the heads on corrupted data while freezing the pre-trained STL/MTL backbone. While this differs from the typical OOD setup, here, it allows us to explore whether MTL or STL yield more robust representation for corrupted data.

We select models trained on clean data with the best performing hyperparameter configuration from previous experiments and fine-tune their heads on corrupted data. Following this, we compare the test performance of models trained in the multi-task setup to those that were learned for a single-task only. We use the perturbation modes proposed by Hendrycks et al. [16] which include different variants of noise, blur, and weather conditions and apply five levels of severity. We randomly select corruption and severity level for each data sample

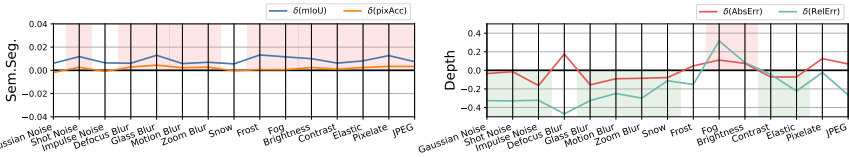


Fig. 5: Transfer to corrupted data for MTL and STL on CityScapes with DeepLabV3 and EW. We show the difference over relative performance decrease over all corruption modes averaged over five levels of severity and three runs. We color blocks if either **STL** or **MTL** can handle the respective corruption better for all metrics of a task. MTL is more robust compared to STL models for the depth task. In contrast, STL deals slightly better on the semantic segmentation task.

Table 3: Out-Of Distribution transfer on corrupted CityScapes [9] for different MTO methods on DeepLabV3. We report difference between relative performance decrease for STL and MTL averaged over all modes of corruption and all levels of severity (Eq. (6)) as well as over runs for three seeds. A value lower than zero indicates a better generalization capability of the MTL backbone and vice versa.

Network	MTO	Sem.Seg.		Depth		Mean
		δ_{mIoU}	δ_{pixAcc}	δ_{AbsErr}	δ_{RelErr}	
DeepLabV3	EW	-0.0087	0.0017	-0.0108	-0.1826	-0.0457
	UW	0.0110	0.0018	0.1179	0.0861	0.0542
	RLW	0.0263	0.0084	-0.0809	-0.3595	-0.1015
	IMTL	0.0172	0.0041	0.1747	0.0857	0.0704
	PCGrad	0.0090	0.0019	0.0394	-0.2240	-0.0434
	CAGrad	0.0224	0.0067	0.0898	-0.2841	-0.0413

during fine-tuning and create a full corrupted version of the test data considering all proposed corruptions and perturbation levels.

To quantify the robustness of single- and multi-task models, we first compute the individual task metrics M (e.g., mIoU) per task t for a STL and MTL network. Next, we compute the relative performance when each model is faced with corrupted data. Lastly, we calculate the difference of relative performances of the MTL compared to the STL model. In detail, over all corruption modes C and levels of severity S we have

$$\delta_t = \frac{1}{|C| \cdot |S|} \sum_{c \in C} \sum_{s \in S} (-1)^{p(t)} \delta_{t,c,s} \quad (6)$$

$$\text{with } \delta_{t,c,s} = \frac{M_{t,c,s}^{\text{MTL,corrupted}}}{M_t^{\text{MTL,clean}}} - \frac{M_{t,c,s}^{\text{STL,corrupted}}}{M_t^{\text{STL,clean}}}$$

where $p(t) = 1$ if a higher value on task t corresponds to better performance and $p(t) = 0$ otherwise. This metric yields $\delta_t < 0$ if the MTL model was able to handle data corruption better. If the STL model is less impacted, we get $\delta_t > 0$.

Results: Figure 5 shows δ_t for different corruption types for a DeepLabV3 with EW on CityScapes averaged over five corruption levels and three seeds. On the semantic segmentation tasks, the STL models show a slightly lower decrease in performance on the corrupted data than MTL ($\delta_t > 0$ more often;

shaded in red), indicating that the features learned for these respective tasks can better generalize to corrupted data. In contrast, the MTL model shows significant better relative performance on the depth task ($\delta_t < 0$ more often; shaded green). Comparing these observations to other dataset+network combinations (Fig. A12), we find a strong robustness of MTL features for both setups of CityScape+SegNet and NYUv2+DeepLabV3 over all tasks. However, evaluation on NYUv2+SegNet resulted on average in better performance on STL features, especially for the depth task. Furthermore, we see little evidence for general higher robustness against certain types of corruption (e.g., higher robustness against weather conditions) for either MTL or STL across all setups.

The results of other MTO methods (Tabs. 3, A8 and A9) indicate that it depends less on the used method but more on the choice of dataset and network architecture whether some tasks would benefit from MTL for learning more robust features. Averaged absolute scores can be found in Tabs. A10 and A11.

Conclusion: Our experiments show that MTL *can* result in learning more robust features, either for a subset of tasks or even all. However, we could not observe a uniform pattern whether certain tasks consistently benefit from MTL. Instead, it depends on the task, the type of corruption, the network, and the dataset whether MTL or STL is superior towards corrupted data. Whether there is a general pattern, we leave to further research. We further cannot fully confirm the outcome of [24] as only two of our setups have indicated that the segmentation task can be more robust in the MTL setting. Controversial to the claim of [37], our evaluation shows that none of the MTL approaches, even IMTL, PC-Grad or CAGrad which adjust the gradients, yields consistent values of $\delta_t < 0$ which would have shown an advantage of certain MTO methods over STL.

5 Conclusion and outlook

This study aims to enhance our understanding of multi-task learning (MTL) in computer vision, providing valuable insights for future research as well as guidance for implementations of real-world applications.

We show that common optimization methods from single task learning (STL) like the Adam optimizer are effective in MTL problems. We explain this with Adam’s partial loss-scale invariance. Next, we compare gradient conflicts during training between tasks and samples. While gradient *magnitudes* are a specific problem between tasks (MTL) and thus justify the need for multi-task specific methods for automatic loss weighting, we find the variability in gradient *alignment* to be similar between samples and tasks. Thus, we encourage a more unified viewpoint in which specific MTO methods are also considered in single-task problems and vice versa. For the ongoing debate regarding the robustness of features from MTL approaches, we find empirical evidence that multi-task features can be more robust than single-task features depending on tasks and setup. Here, future work could try to disentangle the different current perspectives from causal features [17], adversarial/noise robustness [24, 37, 53] and our results on common corruption robustness.

Beyond our work, we encourage research to improve the understanding of challenges and paradigms in MTL. For instance, our understanding of task (and sample) specific capacity allocation within a network and how best to tune it to custom requirements, is still not thoroughly understood. Often task-weights are increased to assign more importance to a task which is in contrast to tuning the learning rate per task where a smaller learning rate can be beneficial. Thus, we require further investigations and disentanglement of these two concepts.

Acknowledgments

We thank Claudia Blaiotta, Martin Rapp, Frank R. Schmidt, Leonhard Henricke, and Bastian Bischoff for their feedback and valuable discussions. Cathrin Elich thanks her supervisors, Jörg Stückler and Marc Pollefeys, for enabling the opportunity to pursue an internship during her Ph.D. studies.

The Bosch Group is carbon neutral. Administration, manufacturing and research activities do no longer leave a carbon footprint. This also includes GPU clusters on which the experiments have been performed.

References

1. Badrinarayanan, V., Kendall, A., Cipolla, R.: SegNet: A Deep Convolutional Encoder-Decoder Architecture for Image Segmentation. *IEEE Transactions on Pattern Analysis and Machine Intelligence* (2017) [5](#), [7](#), [12](#), [13](#)
2. Beery, S., Van Horn, G., Perona, P.: Recognition in terra incognita. In: *Proceedings of the European conference on computer vision (ECCV)*. pp. 456–473 (2018) [12](#)
3. Bernstein, J., Wang, Y.X., Azzadenezsheli, K., Anandkumar, A.: signSGD: Compressed optimisation for non-convex problems. In: Dy, J., Krause, A. (eds.) *Proceedings of the 35th International Conference on Machine Learning. Proceedings of Machine Learning Research*, vol. 80, pp. 560–569. PMLR (10–15 Jul 2018), <https://proceedings.mlr.press/v80/bernstein18a.html> [9](#)
4. Caruana, R.: Multitask learning. *Machine learning* **28**, 41–75 (1997) [1](#), [12](#)
5. Chen, L.C., Zhu, Y., Papandreou, G., Schroff, F., Adam, H.: Encoder-decoder with atrous separable convolution for semantic image segmentation. In: *Computer Vision – ECCV 2018* (2018) [5](#), [7](#), [10](#), [13](#), [14](#)
6. Chen, Z., Badrinarayanan, V., Lee, C., Rabinovich, A.: GradNorm: Gradient normalization for adaptive loss balancing in deep multitask networks. In: Dy, J.G., Krause, A. (eds.) *Proc. of ICML. Proceedings of Machine Learning Research*, vol. 80, pp. 793–802. PMLR (2018), <http://proceedings.mlr.press/v80/chen18a.html> [3](#)
7. Chen, Z., Ngiam, J., Huang, Y., Luong, T., Kretzschmar, H., Chai, Y., Anguelov, D.: Just pick a sign: Optimizing deep multitask models with gradient sign dropout. In: Larochelle, H., Ranzato, M., Hadsell, R., Balcan, M., Lin, H. (eds.) *Advances in Neural Information Processing Systems 33: Annual Conference on Neural Information Processing Systems 2020, NeurIPS 2020, December 6–12, 2020, virtual* (2020), <https://proceedings.neurips.cc/paper/2020/hash/16002f7a455a94aa4e91cc34ebdb9f2d-Abstract.html> [2](#), [3](#)

8. Chennupati, S., Sistu, G., Yogamani, S., A Rawashdeh, S.: Multinet++: Multi-stream feature aggregation and geometric loss strategy for multi-task learning. In: Proceedings of the IEEE/CVF Conference on Computer Vision and Pattern Recognition (CVPR) Workshops (2019) **3**
9. Cordts, M., Omran, M., Ramos, S., Rehfeld, T., Enzweiler, M., Benenson, R., Franke, U., Roth, S., Schiele, B.: The cityscapes dataset for semantic urban scene understanding. In: 2016 IEEE Conference on Computer Vision and Pattern Recognition, CVPR 2016, Las Vegas, NV, USA, June 27-30, 2016. pp. 3213–3223. IEEE Computer Society (2016). <https://doi.org/10.1109/CVPR.2016.350>, <https://doi.org/10.1109/CVPR.2016.350> **5, 7, 13, 9, 10, 12, 20, 21**
10. Désidéri, J.A.: Multiple-gradient descent algorithm (mgda) for multiobjective optimization. *Comptes Rendus Mathématique* **350**, 313–318 (2012) **3**
11. Fernando, H.D., Shen, H., Liu, M., Chaudhury, S., Murugesan, K., Chen, T.: Mitigating gradient bias in multi-objective learning: A provably convergent approach. In: The Eleventh International Conference on Learning Representations, ICLR 2023, Kigali, Rwanda, May 1-5, 2023 (2023) **3**
12. Fifty, C., Amid, E., Zhao, Z., Yu, T., Anil, R., Finn, C.: Efficiently identifying task groupings for multi-task learning. In: Ranzato, M., Beygelzimer, A., Dauphin, Y.N., Liang, P., Vaughan, J.W. (eds.) *Advances in Neural Information Processing Systems 34: Annual Conference on Neural Information Processing Systems 2021, NeurIPS 2021, December 6-14, 2021, virtual*. pp. 27503–27516 (2021), <https://proceedings.neurips.cc/paper/2021/hash/e77910ebb93b511588557806310f78f1-Abstract.html> **3**
13. Geirhos, R., Jacobsen, J.H., Michaelis, C., Zemel, R., Brendel, W., Bethge, M., Wichmann, F.A.: Shortcut learning in deep neural networks. *Nature Machine Intelligence* **2**(11), 665–673 (2020) **12**
14. Guo, M., Haque, A., Huang, D.A., Yeung, S., Fei-Fei, L.: Dynamic task prioritization for multitask learning. In: Proceedings of the European Conference on Computer Vision (ECCV) (2018) **3**
15. He, K., Zhang, X., Ren, S., Sun, J.: Deep residual learning for image recognition. In: 2016 IEEE Conference on Computer Vision and Pattern Recognition, CVPR 2016, Las Vegas, NV, USA, June 27-30, 2016. pp. 770–778. IEEE Computer Society (2016). <https://doi.org/10.1109/CVPR.2016.90>, <https://doi.org/10.1109/CVPR.2016.90> **5, 10**
16. Hendrycks, D., Dietterich, T.G.: Benchmarking neural network robustness to common corruptions and perturbations. In: Proc. of ICLR. OpenReview.net (2019), <https://openreview.net/forum?id=HJz6tiCqYm> **12, 9**
17. Hu, Z., Zhao, Z., Yi, X., Yao, T., Hong, L., Sun, Y., Chi, E.: Improving multi-task generalization via regularizing spurious correlation. *Advances in Neural Information Processing Systems* **35**, 11450–11466 (2022) **12, 14**
18. Ilyas, A., Santurkar, S., Tsipras, D., Engstrom, L., Tran, B., Madry, A.: Adversarial examples are not bugs, they are features. In: Wallach, H.M., Larochelle, H., Beygelzimer, A., d’Alché-Buc, F., Fox, E.B., Garnett, R. (eds.) *Advances in Neural Information Processing Systems 32: Annual Conference on Neural Information Processing Systems 2019, NeurIPS 2019, December 8-14, 2019, Vancouver, BC, Canada*. pp. 125–136 (2019), <https://proceedings.neurips.cc/paper/2019/hash/e2c420d928d4bf8ce0ff2ec19b371514-Abstract.html> **12**
19. Ishihara, K., Kanervisto, A., Miura, J., Hautamäki, V.: Multi-task learning with attention for end-to-end autonomous driving. In: IEEE Conference on Computer Vision and Pattern Recognition Workshops, CVPR Workshops 2021, virtual,

- June 19-25, 2021. pp. 2902–2911. Computer Vision Foundation / IEEE (2021). <https://doi.org/10.1109/CVPRW53098.2021.00325>, https://openaccess.thecvf.com/content/CVPR2021W/WAD/html/Ishihara_Multi-Task_Learning_With_Attention_for_End-to-End_Autonomous_Driving_CVPRW_2021_paper.html 1
20. Javaloy, A., Valera, I.: Rotograd: Gradient homogenization in multitask learning. In: Proc. of ICLR. OpenReview.net (2022), <https://openreview.net/forum?id=T8wHz4rnuGL> 2, 3, 10, 12
 21. Kendall, A., Gal, Y., Cipolla, R.: Multi-task learning using uncertainty to weigh losses for scene geometry and semantics. In: 2018 IEEE Conference on Computer Vision and Pattern Recognition, CVPR 2018, Salt Lake City, UT, USA, June 18–22, 2018. pp. 7482–7491. IEEE Computer Society (2018). <https://doi.org/10.1109/CVPR.2018.00781>, http://openaccess.thecvf.com/content_cvpr_2018/html/Kendall_Multi-Task_Learning_Using_CVPR_2018_paper.html 2, 3, 5, 7, 8, 9, 1, 10
 22. Kingma, D.P., Ba, J.: Adam: A method for stochastic optimization. In: Bengio, Y., LeCun, Y. (eds.) Proc. of ICLR (2015), <http://arxiv.org/abs/1412.6980> 2, 5, 1, 3
 23. Kirchdorfer, L., Elich, C., Kutsche, S., Stuckenschmidt, H., Schott, L., Köhler: Analytical uncertainty-based loss weighting in multi-task learning. unpublished (2023) 8, 1
 24. Klingner, M., Bar, A., Fingscheidt, T.: Improved noise and attack robustness for semantic segmentation by using multi-task training with self-supervised depth estimation. In: Proceedings of the IEEE/CVF Conference on Computer Vision and Pattern Recognition Workshops. pp. 320–321 (2020) 2, 12, 14
 25. Kurin, V., De Palma, A., Kostrikov, I., Whiteson, S., Kumar, M.P.: In Defense of the Unitary Scalarization for Deep Multi-Task Learning. In: Neural Information Processing Systems (2022) 2, 4, 5, 8, 9
 26. Lee, D.G.: Fast drivable areas estimation with multi-task learning for real-time autonomous driving assistant. Applied Sciences 11(22), 10713 (2021) 1
 27. Lin, B., Jiang, W., Ye, F., Zhang, Y., Chen, P., Chen, Y.C., Liu, S., Kwok, J.T.: Dual-balancing for multi-task learning (2023) 3, 8
 28. Lin, B., YE, F., Zhang, Y., Tsang, I.: Reasonable Effectiveness of Random Weighting: A Litmus Test for Multi-Task Learning. Transactions on Machine Learning Research (2022), <https://openreview.net/forum?id=jjtFD8A1Wx> 3, 5, 7, 9, 10
 29. Lin, B., Zhang, Y.: LibMTL: A Python Library for Multi-Task Learning. ArXiv preprint [abs/2203.14338](https://arxiv.org/abs/2203.14338) (2022), <https://arxiv.org/abs/2203.14338> 7, 9, 10
 30. Liu, B., Feng, Y., Stone, P., Liu, Q.: Famo: Fast adaptive multitask optimization. In: Oh, A., Neumann, T., Globerson, A., Saenko, K., Hardt, M., Levine, S. (eds.) Advances in Neural Information Processing Systems. vol. 36, pp. 57226–57243. Curran Associates, Inc. (2023) 3
 31. Liu, B., Liu, X., Jin, X., Stone, P., Liu, Q.: Conflict-averse gradient descent for multi-task learning. In: Ranzato, M., Beygelzimer, A., Dauphin, Y.N., Liang, P., Vaughan, J.W. (eds.) Advances in Neural Information Processing Systems 34: Annual Conference on Neural Information Processing Systems 2021, NeurIPS 2021, December 6-14, 2021, virtual. pp. 18878–18890 (2021), <https://proceedings.neurips.cc/paper/2021/hash/9d27fdf2477ffbf837d73ef7ae23db9-Abstract.html> 2, 3, 5, 6, 7, 10, 12, 9, 11, 16
 32. Liu, L., Li, Y., Kuang, Z., Xue, J., Chen, Y., Yang, W., Liao, Q., Zhang, W.: Towards impartial multi-task learning. In: Proc. of ICLR. OpenReview.net (2021), <https://openreview.net/forum?id=IMPnRXEWpvr> 2, 3, 5, 7, 10

33. Liu, S., James, S., Davison, A.J., Johns, E.: Auto-Lambda: Disentangling Dynamic Task Relationships. *Transactions on Machine Learning Research* (2022) **3**
34. Liu, S., Johns, E., Davison, A.J.: End-to-end multi-task learning with attention. In: *IEEE Conference on Computer Vision and Pattern Recognition, CVPR 2019, Long Beach, CA, USA, June 16-20, 2019*. pp. 1871–1880. Computer Vision Foundation / IEEE (2019). <https://doi.org/10.1109/CVPR.2019.00197>, http://openaccess.thecvf.com/content_CVPR_2019/html/Liu_End-To-End_Multi-Task_Learning_With_Attention_CVPR_2019_paper.html **2, 3, 5, 9, 10**
35. Liu, Z., Luo, P., Wang, X., Tang, X.: Deep learning face attributes in the wild. In: *2015 IEEE International Conference on Computer Vision, ICCV 2015, Santiago, Chile, December 7-13, 2015*. pp. 3730–3738. IEEE Computer Society (2015). <https://doi.org/10.1109/ICCV.2015.425>, <https://doi.org/10.1109/ICCV.2015.425> **5, 9, 10, 17**
36. Maninis, K., Radosavovic, I., Kokkinos, I.: Attentive single-tasking of multiple tasks. In: *IEEE Conference on Computer Vision and Pattern Recognition, CVPR 2019, Long Beach, CA, USA, June 16-20, 2019*. pp. 1851–1860. Computer Vision Foundation / IEEE (2019). <https://doi.org/10.1109/CVPR.2019.00195>, http://openaccess.thecvf.com/content_CVPR_2019/html/Maninis_Attentive_Single-Tasking_of_Multiple_Tasks_CVPR_2019_paper.html **3, 5**
37. Mao, C., Gupta, A., Nitin, V., Ray, B., Song, S., Yang, J., Vondrick, C.: Multi-task learning strengthens adversarial robustness. In: *Computer Vision–ECCV 2020: 16th European Conference, Glasgow, UK, August 23–28, 2020, Proceedings, Part II* 16. pp. 158–174. Springer (2020) **2, 12, 14**
38. Misra, I., Shrivastava, A., Gupta, A., Hebert, M.: Cross-stitch networks for multi-task learning. In: *2016 IEEE Conference on Computer Vision and Pattern Recognition, CVPR 2016, Las Vegas, NV, USA, June 27-30, 2016*. pp. 3994–4003. IEEE Computer Society (2016). <https://doi.org/10.1109/CVPR.2016.433>, <https://doi.org/10.1109/CVPR.2016.433> **3**
39. Nathan Silberman, Derek Hoiem, P.K., Fergus, R.: Indoor segmentation and support inference from rgb-d images. In: *ECCV (2012)* **5, 7, 9, 10, 13, 14, 21, 23**
40. Navon, A., Shamsian, A., Achituve, I., Maron, H., Kawaguchi, K., Chechik, G., Fetaya, E.: Multi-task learning as a bargaining game. In: Chaudhuri, K., Jegelka, S., Song, L., Szepesvári, C., Niu, G., Sabato, S. (eds.) *International Conference on Machine Learning, ICML 2022, 17-23 July 2022, Baltimore, Maryland, USA. Proceedings of Machine Learning Research*, vol. 162, pp. 16428–16446. PMLR (2022), <https://proceedings.mlr.press/v162/navon22a.html> **3**
41. Pascal, L., Michiardi, P., Bost, X., Huet, B., Zuluaga, M.A.: Improved optimization strategies for deep multi-task networks. *ArXiv preprint abs/2109.11678* (2021), <https://arxiv.org/abs/2109.11678> **3, 7, 4**
42. Royer, A., Blankevoort, T., Bejnordi, B.E.: Scalarization for multi-task and multi-domain learning at scale. In: *Thirty-seventh Conference on Neural Information Processing Systems (2023)* **4, 12**
43. Ruder, S.: An overview of multi-task learning in deep neural networks. *ArXiv preprint abs/1706.05098* (2017), <https://arxiv.org/abs/1706.05098> **3**
44. Sener, O., Koltun, V.: Multi-task learning as multi-objective optimization. In: Bengio, S., Wallach, H.M., Larochelle, H., Grauman, K., Cesa-Bianchi, N., Garnett, R. (eds.) *Advances in Neural Information Processing Systems 31: Annual Conference on Neural Information Processing Systems 2018, NeurIPS 2018, December 3-8, 2018, Montréal, Canada*. pp. 525–536 (2018), <https://proceedings.neurips.cc/paper/2018/hash/432aca3a1e345e339f35a30c8f65edce-Abstract.html> **3, 6**

45. Senushkin, D., Patakin, N., Kuznetsov, A., Konushin, A.: Independent component alignment for multi-task learning. In: IEEE/CVF Conference on Computer Vision and Pattern Recognition, CVPR 2023, Vancouver, BC, Canada, June 17-24, 2023. IEEE (2023) [3](#), [5](#), [7](#), [10](#)
46. Shi, G., Li, Q., Zhang, W., Chen, J., Wu, X.M.: Recon: Reducing Conflicting Gradients From the Root For Multi-Task Learning. In: The Eleventh International Conference on Learning Representations (2023) [3](#), [10](#)
47. Standley, T., Zamir, A.R., Chen, D., Guibas, L.J., Malik, J., Savarese, S.: Which tasks should be learned together in multi-task learning? In: Proc. of ICML. Proceedings of Machine Learning Research, vol. 119, pp. 9120–9132. PMLR (2020), <http://proceedings.mlr.press/v119/standley20a.html> [3](#)
48. Vandenhende, S., Georgoulis, S., Van Gansbeke, W., Proesmans, M., Dai, D., Van Gool, L.: Multi-task learning for dense prediction tasks: A survey. IEEE Transactions on Pattern Analysis and Machine Intelligence (2021). <https://doi.org/10.1109/TPAMI.2021.3054719> [2](#), [3](#)
49. Xin, D., Ghorbani, B., Garg, A., Firat, O., Gilmer, J.: Do Current Multi-Task Optimization Methods in Deep Learning Even Help? In: Neural Information Processing Systems (2022) [2](#), [3](#), [5](#), [6](#), [8](#), [9](#), [12](#), [4](#)
50. Xu, D., Ouyang, W., Wang, X., Sebe, N.: Pad-net: Multi-tasks guided prediction-and-distillation network for simultaneous depth estimation and scene parsing. In: 2018 IEEE Conference on Computer Vision and Pattern Recognition, CVPR 2018, Salt Lake City, UT, USA, June 18-22, 2018. pp. 675–684. IEEE Computer Society (2018). <https://doi.org/10.1109/CVPR.2018.00077>, http://openaccess.thecvf.com/content_cvpr_2018/html/Xu_PAD-Net_Multi-Tasks_Guided_CVPR_2018_paper.html [3](#)
51. Yang, E., Pan, J., Wang, X., Yu, H., Shen, L., Chen, X., Xiao, L., Jiang, J., Guo, G.: Adatask: A task-aware adaptive learning rate approach to multi-task learning. Proceedings of the AAAI Conference on Artificial Intelligence **37**(9), 10745–10753 (2023) [3](#), [7](#), [9](#), [4](#)
52. Ye, F., Lin, B., Yue, Z., Guo, P., Xiao, Q., Zhang, Y.: Multi-objective meta learning. In: Advances in Neural Information Processing Systems. vol. 34 (2021) [3](#)
53. Yeo, T., Kar, O.F., Zamir, A.: Robustness via cross-domain ensembles. In: 2021 IEEE/CVF International Conference on Computer Vision, ICCV 2021, Montreal, QC, Canada, October 10-17, 2021. pp. 12169–12179. IEEE (2021). <https://doi.org/10.1109/ICCV48922.2021.01197>, <https://doi.org/10.1109/ICCV48922.2021.01197> [12](#), [14](#)
54. Yu, F., Koltun, V., Funkhouser, T.A.: Dilated residual networks. In: 2017 IEEE Conference on Computer Vision and Pattern Recognition, CVPR 2017, Honolulu, HI, USA, July 21-26, 2017. pp. 636–644. IEEE Computer Society (2017). <https://doi.org/10.1109/CVPR.2017.75>, <https://doi.org/10.1109/CVPR.2017.75> [10](#)
55. Yu, T., Kumar, S., Gupta, A., Levine, S., Hausman, K., Finn, C.: Gradient surgery for multi-task learning. In: Larochelle, H., Ranzato, M., Hadsell, R., Balcan, M., Lin, H. (eds.) Advances in Neural Information Processing Systems 33: Annual Conference on Neural Information Processing Systems 2020, NeurIPS 2020, December 6-12, 2020, virtual (2020), <https://proceedings.neurips.cc/paper/2020/hash/3fe78a8acf5fda99de95303940a2420c-Abstract.html> [2](#), [3](#), [5](#), [6](#), [7](#), [10](#), [11](#), [12](#)
56. Zhao, H., Shi, J., Qi, X., Wang, X., Jia, J.: Pyramid scene parsing network. In: 2017 IEEE Conference on Computer Vision and Pattern Recognition, CVPR 2017, Honolulu, HI, USA, July 21-26, 2017. pp. 6230–6239. IEEE Computer Society (2017). <https://doi.org/10.1109/CVPR.2017.660>, <https://doi.org/10.1109/CVPR.2017.660> [10](#)

Challenging Common Paradigms in Multi-Task Learning -Supplementary Material-

A1 Theoretical insights into multi-task learning dynamics

In this section, we aim to explain the success of the Adam optimizer [22] by relating it to uncertainty weighting [21]. We show partial invariances w.r.t. prior task-weights for the Adam optimizer and full invariances for the uncertainty weighting under mild assumptions. We further show that for SGD + momentum no invariance can be observed. Instead, the loss-weight can be seen as a task-specific learning rate which is not the case for the Adam optimizer. Previous literature on weighting methods in MTL did not explicitly show how task-weighting methods are affected by different optimizers.

A1.1 Uncertainty weighting (UW): Full loss-scale invariance

In UW [21], the homoscedastic uncertainty⁵ σ_t to weight task t is learned by gradient descent. However, we can also analytically compute the optimal uncertainty weights in each iteration instead of learning them using gradient descent as done in [23]. The minimization objective depends on the underlying loss function and likelihood. For simplicity, we show the derivation exemplary for the L_1 loss. It is straight-forward to derive the same for a Gaussian and other distributions. The objective of uncertainty weighting is given as

$$\min_{\sigma_t} \frac{1}{\sigma_t} \mathcal{L}_t + \log \sigma_t \quad (7)$$

with $\mathcal{L}_t = |y - f^W(x)|$ which can be derived from a log likelihood of a Laplace distribution $p(y|f^W(x), \sigma) = \frac{1}{2\sigma} \exp(-\frac{|y-f^W(x)|}{\sigma})$. Taking the derivative and solving for σ_t results in an analytically optimal solution:

$$\frac{\partial}{\partial \sigma_t} \frac{1}{\sigma_t} \mathcal{L}_t + \log \sigma_t = -\frac{1}{\sigma_t^2} \mathcal{L}_t + \frac{1}{\sigma_t} \quad (8)$$

$$-\frac{1}{\sigma_t^2} \mathcal{L}_t + \frac{1}{\sigma_t} \stackrel{!}{=} 0 \quad \Rightarrow \quad \sigma_t = \mathcal{L}_t \quad (9)$$

with $\sigma_t > 0$. As the optimization problem is convex and just one dimensional, assuming an optimal log-sigma is a mild assumption. Plugging the optimal solution back into the original uncertainty weighting, we get

$$\mathcal{L} = \sum_t \frac{1}{sg[\mathcal{L}_t]} \mathcal{L}_t + \log \sqrt{sg[\mathcal{L}_t]}, \quad (10)$$

where we denote sg as the stopgradient operator.

Since there is no gradient for the second part of the loss, it can be simplified such that

⁵ In Kendall et al., this is termed the aleatoric homoscedastic uncertainty. However, as the task weights vary over the course of training and also with respect to the model capacity, it is technically not only the aleatoric uncertainty but also encapsulates further components such as model capacity and amount of data seen.

$$\mathcal{L} = \sum_t \frac{\mathcal{L}_t}{sg[\mathcal{L}_t]}. \quad (11)$$

Assuming task-specific weights α_t , we get

$$\mathcal{L} = \sum_t \frac{\alpha_t \mathcal{L}_t}{\alpha_t sg[\mathcal{L}_t]} = \sum_t \frac{\mathcal{L}_t}{sg[\mathcal{L}_t]} \quad (12)$$

Therefore, the optimal uncertainty weighting is invariant w.r.t. task-specific loss-scalings, as each scaling cancels out.

A1.2 SGD: No loss-scale invariance and relationship of learning rate and task weights on a gradient level

Unlike for optimal UW, we show that the SGD update rule does not show any invariances and that task-weights are essentially task-specific learning rates. Instead, task-weights and learning rate are interacting hyperparameters and thus cannot be viewed in isolation.

The parameter update rule in neural networks optimized with SGD is

$$\theta_i = \theta_{i-1} - \gamma \frac{\partial}{\partial \theta_{i-1}} \mathcal{L}, \quad (13)$$

where the network parameters in iteration i are defined as θ_i , γ is the learning rate and $\mathcal{L} = \sum_t \alpha_i \mathcal{L}_t$.

In the case of uniform task weights (EW), $\alpha = \alpha_i \forall i$, we have

$$\begin{aligned} \theta_i &= \theta_{i-1} - \gamma \frac{\partial}{\partial \theta_{i-1}} \sum_i \alpha \mathcal{L}_t \\ &= \theta_{i-1} - \gamma \alpha \frac{\partial}{\partial \theta_{i-1}} \sum_i \mathcal{L}_t \end{aligned} \quad (14)$$

Here, task weight and learning rate are interchangeable. In particular, increasing the weight α by a constant factor c has the same effect as increasing the learning rate by a factor c .

In the case of non-uniform task weights α_i , the parameter update is

$$\begin{aligned} \theta_i &= \theta_{i-1} - \gamma \frac{\partial}{\partial \theta_{i-1}} \sum_i \alpha_i \mathcal{L}_t \\ &= \theta_{i-1} - \frac{\partial}{\partial \theta_{i-1}} \sum_i \gamma \alpha_i \mathcal{L}_t \end{aligned} \quad (15)$$

As the learning rate can be included in the task-specific weight, it follows that task weighting is interchangeable to assigning *task-specific* learning rates. Tasks with a higher weight α_i have a proportionally higher parameter update step and vice versa.

While this holds for SGD and SGD + momentum, it does not apply to optimizers such as Adam, Adagrad, or RMSProp. We demonstrate this for Adam in the following subsection.

A1.3 Adam: Partial loss-scale invariance

Similarly to the invariance demonstrated for optimal UW, we derive a partial invariance for Adam. In their work, Kingma and Ba [22] have already shown that the magnitudes of the parameter updates using Adam are invariant to rescaling the gradients. Our novelty lies in demonstrating this invariance property in the context of MTL and its impact on different MTO methods. For Adam, we claim that the magnitude of task-specific weights only affects the backbone and cancels out for the heads.

We consider the standard MTL model setting with a shared backbone and task-specific heads. In this analysis, we assume a frozen backbone and only look at the task-specific parameters ψ_t of task t whose loss \mathcal{L}_t is scaled by α_t , such that $\mathcal{L}_t \rightarrow \alpha_t \mathcal{L}_t$. The parameter update of one head is independent of the other heads as the derivative of the losses w.r.t. the other tasks is 0:

$$\frac{\partial}{\partial \psi_{t,i-1}} \mathcal{L}_j = 0 \text{ for } t \neq j. \quad (16)$$

The general update rule for parameters ψ at time step i using Adam is

$$\psi_i = \psi_{i-1} - \frac{\gamma}{\sqrt{\hat{v}_i} + \epsilon} \hat{m}_i, \quad (17)$$

where $m_i = \beta_1 m_{i-1} + (1 - \beta_1) g_i$ and $v_i = \beta_2 v_{i-1} + (1 - \beta_2) g_i^2$. To counteract the bias towards 0, the moments are corrected as $\hat{m}_i = \frac{m_i}{1 - \beta_1^i}$ and $\hat{v}_i = \frac{v_i}{1 - \beta_2^i}$.

For task-specific parameters ψ_t , task weights α_t linearly scale the first moment $m_{t,i}$

$$\begin{aligned} m_{t,i} &= \beta_1 m_{t,i-1} + (1 - \beta_1) g_{t,i} \\ &= \beta_1 m_{t,i-1} + (1 - \beta_1) \frac{\partial}{\partial \psi_{t,i-1}} \alpha_t \mathcal{L}_t \\ &= \beta_1 m_{t,i-1} + (1 - \beta_1) \alpha_t \frac{\partial}{\partial \psi_{t,i-1}} \mathcal{L}_t \\ &= \beta_1 m_{t,i-1} + (1 - \beta_1) \alpha_t g'_{t,i} \end{aligned} \quad (18)$$

and quadratically scale the second moment $v_{t,i}$

$$\begin{aligned} v_{t,i} &= \beta_2 v_{t,i-1} + (1 - \beta_2) g_{t,i}^2 \\ &= \beta_2 v_{t,i-1} + (1 - \beta_2) \left(\frac{\partial}{\partial \psi_{t,i-1}} \alpha_t \mathcal{L}_t \right)^2 \\ &= \beta_2 v_{t,i-1} + (1 - \beta_2) \alpha_t^2 \left(\frac{\partial}{\partial \psi_{t,i-1}} \mathcal{L}_t \right)^2 \\ &= \beta_2 v_{t,i-1} + (1 - \beta_2) \alpha_t^2 g'^2_{t,i}, \end{aligned} \quad (19)$$

where $g'_{t,i}$ is the gradient of the unscaled loss \mathcal{L}_t w.r.t. the task-specific parameters for task t . As this holds for iteration i and because we have $m_{t,1} = \alpha_t g'_{t,1} + 0$ respectively $v_{t,1} = \alpha_t^2 g'^2_{t,1} + 0$ with $m_{t,0} = 0$, $v_{t,0} = 0$ at the first iteration, this holds for any iteration step. We can thus rewrite $\hat{m}_{t,i} = \alpha_t \hat{m}'_{t,i}$ and $\hat{v}_{t,i} = \alpha_t^2 \hat{v}'_{t,i}$.

Plugging this back into the update rule, we get

$$\begin{aligned}\psi_{t,i-1} &= \psi_{t,i-1} - \frac{\gamma}{\sqrt{\hat{v}_{t,i}}} \hat{m}_{t,i} \\ &= \psi_{t,i-1} - \frac{\gamma}{\sqrt{\alpha_t \hat{v}'_{t,i}}} \alpha_t \hat{m}'_{t,i}\end{aligned}\tag{20}$$

where the loss-scaling α_t cancels out. Therefore, the parameters of the task-specific heads are invariant to loss-scalings using Adam.

This partial invariance is a highly desired property as there is a fundamental trade-off between tuning the learning rate and manual task weights. Given Adams invariance for the head, the weighting only affects the backbone. Thus the learning rate can be set for the parameters of the head independent of the loss weights. With the loss weights, we can prioritize tasks in the backbone and therefore walk along the Pareto front as empirically shown by [49].

The invariance, however, does not hold anymore when the backbone parameters θ are updated as well. As we have

$$\begin{aligned}m_i &= \beta_1 m_{i-1} + (1 - \beta_1) \frac{\partial}{\partial \theta_{i-1}} \sum_t \alpha_t \mathcal{L}_t \\ &= \beta_1 m_{i-1} + (1 - \beta_1) \sum_t \alpha_t g'_{t,i}\end{aligned}\tag{21}$$

and

$$\begin{aligned}v_i &= \beta_1 v_{i-1} + (1 - \beta_1) \left(\frac{\partial}{\partial \theta_{i-1}} \sum_t \alpha_t \mathcal{L}_t \right)^2 \\ &= \beta_1 v_{i-1} + (1 - \beta_1) \left(\sum_t \alpha_t g'_{t,i} \right)^2\end{aligned}\tag{22}$$

we conclude that the task weights a_t linearly affect the first moment m_i , while having a quadratic effect on the update of the second moment v_i .

Note that for both task-heads only as well as the backbone, we have a full invariance in case of independent optimizers, e.g., one Adam optimizer per task similar to [41, 51]. However, naive implementations scale poorly (in terms of computational complexity) with the number of tasks here.

In the following experiments, we provide empirical evidence for our finding that a) Adam offers loss-scale invariance for the parameters of the task-specific heads, and b) Adam offers loss-scale invariance for all network parameters (backbone and heads) if $\beta_{1,2} = 0$.

A2 Empirical Confirmation of scale invariances in Adam and Optimal Uncertainty Weighting

In the prior section, we derived theoretical results for loss-scale (partial) invariance within multi-task learning for the Adam optimizer and uncertainty weighting. In this section, we confirm this invariance empirically with a toy task.

Experimental Setup We consider a two-task toy experiment in which we look at the gradient magnitudes with different combinations of Adam, SGD, EW, optimal uncertainty weighting (UW-O), and loss-scalings. To generate the data, we sample scalar input values from a uniform distribution; the outputs are just scalings of the input. We apply a simple neural network which consists of a shared backbone (two layers with LeakyReLU as non-linearity and 20 neurons per hidden layer) and two heads for the two tasks, each consisting again of two layers. Both task measure the depth but in different units using the L_1 -loss.

We provide two settings: In the first one, depth is measured on the same scale. In the second setting, one depth loss is scaled by 10x (e.g., measured in cm instead of deci-meters) and one other loss is scaled by 0.1 (e.g., measured in meters instead of deci-meters). For each setting, we test various combinations of loss weighting and optimizer combinations.

The 8 different experiments are:

- EW using SGD
- EW using SGD with scalings $10 \cdot L_{seg}$, $0.01 \cdot L_{dep}$
- EW using Adam
- EW using Adam with scalings $10 \cdot L_{seg}$ and $0.01 \cdot L_{dep}$
- UW-O) using SGD
- UW-O) using SGD with scalings $10 \cdot L_{seg}$ and $0.01 \cdot L_{dep}$
- EW using separate Adam optimizers per task
- EW using separate Adam optimizers per task with scalings $10 \cdot L_{seg}$, $0.01 \cdot L_{dep}$

To better control for different factors of influence, we first perform the first 6 of the listed experiments with a fixed backbone, i.e., we do not update the parameters in the backbone but only in the heads. Afterward, we show all 8 experiments trained with a network where all parameters (including the backbone) are updated. This allows us to verify if our theoretical derivations regarding the (partial) loss-scaling invariance of Adam and UW-O also hold in practice, and compare this to the SGD optimizer.

Note that we only care about the invariance and did not tune any hyperparameters for performance.

Results for fixed backbone Figure A1 shows the losses, the scaled losses (by loss weighting method), the gradient magnitudes as well as the gradient update magnitudes for both heads along the 100 epochs of training with a fixed backbone. Regarding SGD, we can observe that the equal weighting experiment differs from its scaled variant along all 8 dimensions. This is because SGD does not offer any loss-scaling invariance. As expected, at the beginning of the training the gradient update magnitude of the first depth head parameters with the scaled loss (dotted line) is by a factor of 10 higher than the unscaled (solid line) one. The same effect applies to the gradient update magnitude of the second depth head parameters, but with a factor of 0.01.

In contrast, Adam is loss-scale invariant. We can observe that the unscaled (solid line) and the scaled version (dotted line) have equal gradient update magnitudes in the last row. Note that practically due to an $\epsilon = 10^{-8}$ parameter in the denominator and float precision a slight divergence would occur with larger number of epochs. This result confirms our theoretical finding in equation 20. We skip the experiment of separated Adam optimizers per task because it would be equivalent to this version given a fixed backbone.

Lastly, we want to investigate the invariance properties of UW-O. We compare the scaled (dotted line) and unscaled (solid line) version of UW-O with the SGD optimizer. As expected, the gradients, as well as the gradient updates, match in both heads.

In the following, let’s investigate whether the observed results still hold if we also consider the update of the backbone parameters.

Results for free backbone Figure A2 shows the scaled losses, the gradient magnitudes as well as the gradient update magnitudes in the backbone and the depth heads along the 100 epochs of training with a free backbone. Again, the loss-scalings affect the gradient magnitudes using SGD. This applies to both backbone and heads.

When looking at the Adam experiments, we can observe that it is partly loss-scale invariant by looking at the first iteration in the heads. However, due to different updates in the backbone, the networks behave different in both settings (scaled and unscaled losses). Furthermore, when implementing task-specific optimizers, we can observe that not only the gradient update magnitudes in the task heads, but also in the backbone match between the scaled (dotted line) and the unscaled (solid line) variant. Thus, all network parameters are invariant to loss-scalings when using separate Adam optimizers. This confirms our theoretical results.

Along the lines of our theoretical findings, we can observe that UW-O offers scaling-invariance across the whole network as the gradients as well as the gradient updates match among the two variants in the backbone and in both heads. This empirical observation matches our theoretical derivation in equation 12.

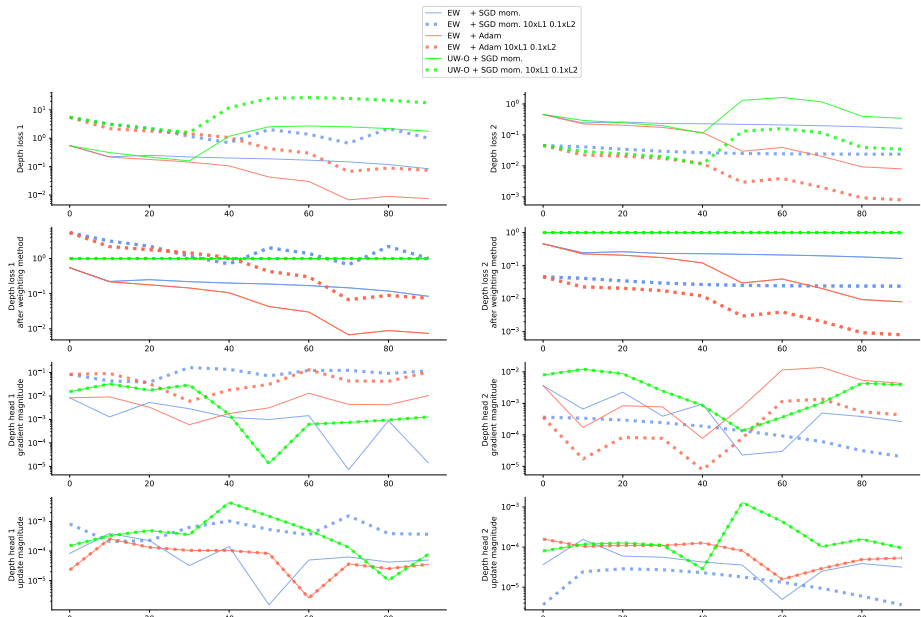


Fig. A1: Invariances within the neural network for a frozen backbone. Comparing the effect of loss-scalings in a toy experiment with two tasks. For each optimizer and loss weighting combination, we run two settings with a) loss L1 and loss L2 are equally weighted or b) L1 is scaled by 10x and L2 by 0.1. For each setting, we measure the scaled losses, gradient magnitudes, and gradient update magnitudes in the the two task heads and keep the backbone frozen. While SGD does not offer any loss-scaling invariance, Adam makes the gradient updates of the head parameters invariant to scales confirming our derivation (red lines overlap in lowest row). Equivalently, for UW-O we also observe the theoretically derived invariances (green lines overlap in lowest row)

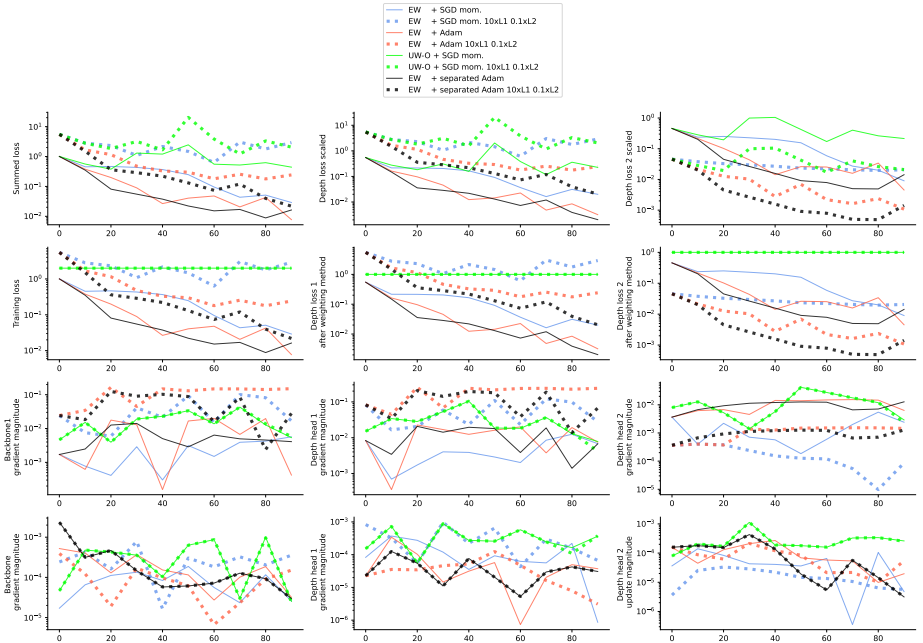


Fig. A2: Invariances within the neural network for a learnable backbone.

Comparing the effect of loss-scalings in a toy experiment with two tasks. For each optimizer and loss weighting combination, we run two settings with a) loss L1 and loss L2 are equally weighted or b) L1 is scaled by 10x and L2 by 0.1. For each setting, we measure the SGD + momentum and Adam optimizer with no post weighting (EW) and SGD + momentum with optimal uncertainty weighting. Additionally, we implement independent Adam optimizer per task. We show the scaled losses, gradient magnitudes, and gradient update magnitudes in the backbone (first row) and the two task heads (2nd and 3rd row). Neither Adam, nor SGD show invariances if the backbone is trained as well. UW-O is still invariant (green lines are overlapping). We revoke Adam's invariance by implementing separate optimizers per task (lowest black lines are overlapping).

A3 Implementation Details

In this section, we explain the applied settings used for the reported experiments in more detail. In particular, we describe the handling of the different datasets in Appendix A3.1 and provide further information on the applied training procedures in Appendix A3.2. Our chosen experimental setups are designed to follow previous work and mainly inspired by [29, 31, 49]. However, we found that the experimental setup would vary widely across different works in the field of multi-task learning as can be seen in Table A1. We use a uniform setup for each dataset independent of the choice of network and MTO.

A3.1 Datasets

CityScapes [9] We make use of the official split of the dataset which consists of 2975 training and 500 validation scenes. Similar to [49], we denote 595 random samples from the training split as validation data and report test results on the original validation split. We further follow the pre-processing scheme from [34] of re-scaling images to 128x256 pixels and use inverse depth labels. During training, we apply random scaling and cropping for data augmentation⁶. Following previous work [31] for number of epochs and learning rate schedule, we train for 300 epochs and decrease the learning rate by a factor of 0.5 every 100 epochs. The batch size is set to 64, similar to [49]. We only consider a fixed weight decay of 10^{-5} for all datasets and experiments as we found varying this parameter had only little influence in initial experiments.

NYUv2 [39] From the 795 official training images we use 159 for our validation split as in [29] and report test performance on the official 654 test images. Similar to [34], we re-size the images to 288x384 pixels. Training is run for 200 epochs with a batch size of 8. We apply the same data augmentation and learning rate schedule as for CityScapes.

CelebA [35] We re-size images to 64x64 pixels as done in [28] and consider the original split of 162,770/19,867/19,962 for training, validation, and testing. We set the batch size to 512, train for 100 epochs, and halve the learning rates every 30 epochs.

Corrupted variants For Cityscapes and NYUv2 we apply the common corruptions proposed by [16]. We use their original code⁷.

A3.2 Training

Effectiveness of Adam in MTL. All presented results are based on performing early stopping w.r.t. Δ_m - metric on the validation set. For this, we further trained single-task learning (STL) models for each experiment combination

⁶ <https://github.com/Cranial-XIX/CAGrad>

⁷ <https://github.com/hendrycks/robustness>

Table A1: Original experiment setup as reported in respective papers. We note a high variation regarding the choice of network, optimizer, and other hyper-parameters among the different works.

Data MTO	Network	Optimizer	learning rate	weight decay	batch size	#train. iterations	
CityScapes [9]	UW [21]	DeepLabV3 [5] with ResNet101 [54]	SGD + Nesterov updates, Mom.	init.: $2.5 \cdot 10^{-3}$; polynomial lr decay	$1 \cdot 10^{-4}$	8	100k iter.
	RLW [28]	DeepLabV3 [5] with ResNet50 [54]	Adam	$1 \cdot 10^{-4}$	$1 \cdot 10^{-5}$	64	
	IMTL [32]	ResNet50 [54] + PSPNet [56] heads	SGD+Mom.	init.: 0.02; polynomial lr decay	$1 \cdot 10^{-4}$	32	200 epochs
	PCGrad [55]	MTAN [34]	Adam	init.: $1 \cdot 10^{-4}$; halve lr after 40k iter.	-	8	80k iter
	CAGrad [31]	MTAN [34]	Adam	init.: $1 \cdot 10^{-4}$; halve lr every 100 epochs	-	8	200 epochs
	AlignedMTL [45]	MTAN [34] / PSPNet [56]	Adam	init.: $1 \cdot 10^{-4}$; halve lr every 100 epochs	-	8	200 epochs
NYUv2 [39]	RLW [28]	DeepLabV3 [5] with ResNet50 [54]	Adam	$1 \cdot 10^{-4}$	$1 \cdot 10^{-5}$	8	
	IMTL [32]	ResNet50 [54] + PSPNet [56] heads	SGD+Mom.	init.: 0.03	-	48	200 epochs
	PCGrad [55]	MTAN [34]	Adam	init.: $1 \cdot 10^{-4}$; halve lr after 40k iter.	-	2	80k iter
	CAGrad [31]	MTAN [34]	Adam	init.: $1 \cdot 10^{-4}$; halve lr after 100 epochs	-	2	200 epochs
	AlignedMTL [45]	MTAN [34] / PSPNet [56]	Adam	init.: $1 \cdot 10^{-4}$; halve lr after 100 epochs	-	2	200 epochs
CelebA [35]	RLW [28]	ResNet17 [15] + lin. classifier	Adam	$1 \cdot 10^{-3}$	-	512	
	IMTL [32]	ResNet17 [15] + lin. classifier	Adam	0.003	-	256	100 epochs
	PCGrad [55]	ResNet17 [15] + lin. classifier	Adam	init. from $\{10^{-4}, \dots, 5 \cdot 10^{-2}\}$; halve lr every 30 epochs	-	256	100 epochs

(dataset and network) using the respective network architecture except for the missing head(s). We trained the models using Adam and any learning rate from $\{0.01, 0.005, \dots, 0.00005\}$. The training was stopped early based on the validation loss. Reported scores in Tabs. A3 to A6 are computed as the mean of the models’ performance that were initialized with the three different seeds.

Our implementation for all experiments is based on the LibMTL library [29].

Gradient Similarity. Our gradient similarity experiments were conducted on the best performing hyper-parameter configuration for EW from the previous extensive evaluation. Over the full training, gradient similarity measures are computed every five iteration steps and summarized per epoch. To make the computation effort more feasible in case of settings with large batch size or high number of tasks, we randomly select eight samples or tasks respectively and consider corresponding gradients in these cases.

A4 Additional results on comparison between Adam and SGD

We present additional evaluation results for our comparison between optimizers for MTL. In Figure A3, we compare the Δ_m -metric performance between the usage of Adam and SGD+mom. Fig. A4 shows additional parallel coordinate plots for NYUv2 and both choices of networks. In Table A2, we count for each used MTO method the number of experiment runs that are located on the Pareto front w.r.t. each setup. Best performing quantitative results for all MTOs can be found in Tabs. A3 to A6.

We further show extended results on the toy task by Liu et al. [31] for more learning rates in Fig. A5 and Tab. A7.

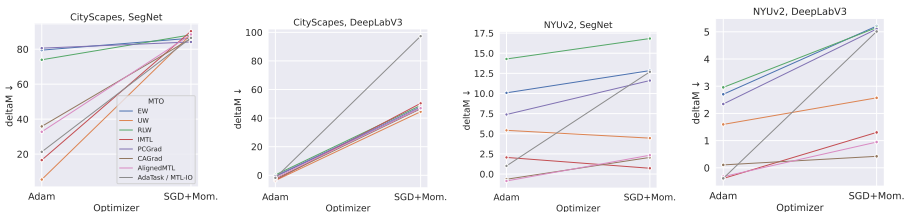


Fig. A3: Mean Δ_m -metric for experiments run on CityScapes and NYUv2 with SegNet and DeepLabV3. We compare the performance of the best hyperparameter setting for every MTO method using either Adam (left) or SGD+Momentum (right) (lower is better). Every MTO is associated with a different line color/style. On Cityscapes, there is a large difference for the Δ_m score for Adam compared to SGD+Momentum, especially for UW, IMTL, and CAGrad. Therefore, for this setup, the result depends more on the optimizer than on the MTO method. On the NYUv2 dataset this observation weakens. Adam still achieves the lowest Δ_m scores across different MTO methods (except for SegNet with UW and IMTL), though, besides choosing Adam, it is also important to select the appropriate MTO method.

Table A2: Count of Pareto optimal experiments for each MTO method. We found no single MTO method to be clearly superior over all combinations of dataset and networks. Total numbers can be compared to Table 2

Data	Network	Optimizer	EW	UW	RLW	IMTL	PCGrad	CAGrad	AlignedMTL	AdaTask	Total
CityScapes	SegNet	Adam	-	3	-	-	-	1	1	-	5
CityScapes	SegNet	SGD+Mom.	-	-	-	-	-	-	-	-	-
CityScapes	DeepLabV3	Adam	2	2	1	2	2	1	-	-	15
CityScapes	DeepLabV3	SGD+Mom.	-	-	-	-	-	-	-	-	-
NYUv2	SegNet	Adam	1	2	-	1	1	1	3	2	11
NYUv2	SegNet	SGD+Mom.	-	-	-	1	-	-	-	-	1
NYUv2	DeepLabV3	Adam	2	-	1	3	3	2	2	3	16
NYUv2	DeepLabV3	SGD+Mom.	-	1	-	-	-	3	2	-	6

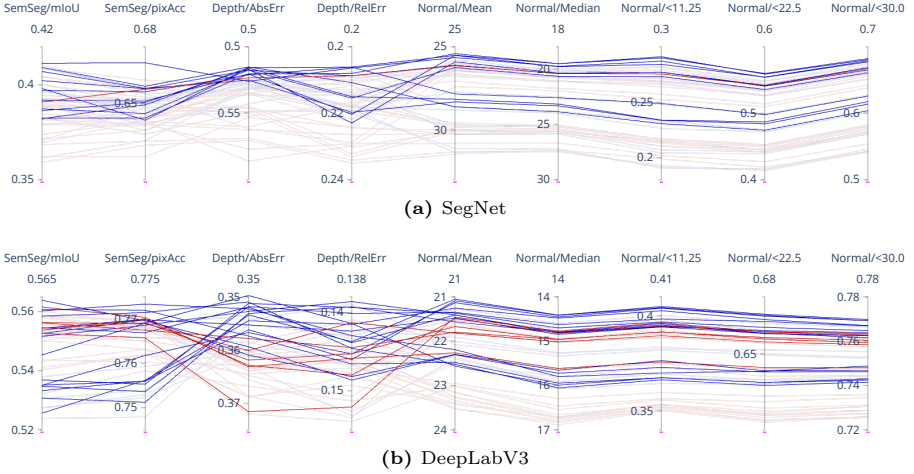


Fig. A4: Parallel coordinate plot over all experiments on NYUv2. We distinguish between experiments using **SGD+mom** and **Adam** optimizer. Experiments that reached Pareto front performance are drawn with higher saturation.

Similar to results on CityScapes in the main paper (Fig. 2) we observe a dominance of Adam albeit, here, we also have some experiments using SGD+Mom. on the overall Pareto front.

Table A3: Results for different MTO methods and optimizers on CityScapes [9] using SegNet [1]. The best score per metric is highlighted for each MTO method as well as over all methods and optimizers. While different MTO methods perform best over the distinct metrics, models trained with Adam outperform those based on SGD+mom in most direct comparisons. On the overall Δ_m -metric, Adam shows superior performance for all MTO methods, in some cases even with a high margin. Best performance for each metric was also achieved by using Adam.

MTO	Optimizer	lr	Sem.Seg.		Depth		DeltaM ↓
			mIoU ↑	pixAcc ↑	AbsErr ↓	RelErr ↓	
STL	adam		0.7122	0.9221	0.0134	29.88	
EW	adam	0.005	0.6898	0.9165	0.0196	109.84	79.43 ±3.68
EW	signSGD	0.001	0.7013	0.9174	0.0210	115.67	86.52 ±6.06
EW	sgd	0.1	0.6967	0.9179	0.0216	113.82	86.24 ±1.97
UW	adam	0.001	0.7052	0.9202	0.0136	35.69	5.44 ±2.38
UW	signSGD	0.001	0.6506	0.8997	0.0166	53.61	28.54 ±7.83
UW	sgd	0.1	0.6750	0.9110	0.0219	114.67	88.39 ±1.35
RLW	adam	0.001	0.7013	0.9196	0.0197	103.61	73.91 ±7.63
RLW	signSGD	0.0005	0.6962	0.9169	0.0204	112.46	82.90 ±5.32
RLW	sgd	0.1	0.6918	0.9156	0.0227	113.59	88.16 ±0.67
IMTL	adam	0.005	0.6963	0.9170	0.0148	45.63	16.55 ±1.52
IMTL	signSGD	0.005	0.6659	0.9070	0.0197	101.90	74.03 ±14.62
IMTL	sgd	0.1	0.6716	0.9107	0.0230	114.38	90.21 ±0.74
PCGrad	adam	0.01	0.6770	0.9135	0.0226	103.88	80.56 ±3.70
PCGrad	signSGD	0.001	0.6929	0.9170	0.0210	113.32	84.74 ±3.46
PCGrad	sgd	0.1	0.6972	0.9176	0.0235	107.06	84.09 ±0.93
CAGrad	adam	0.001	0.7088	0.9208	0.0162	66.39	35.81 ±14.91
CAGrad	signSGD	0.001	0.6883	0.9138	0.0182	107.06	74.68 ±18.91
CAGrad	sgd	0.1	0.6896	0.9156	0.0205	115.52	85.88 ±0.31
AlignedMTL	adam	0.0005	0.7164	0.9246	0.0154	64.89	32.76 ±5.27
AlignedMTL	signSGD	0.001	0.7010	0.9189	0.0180	102.41	69.77 ±24.91
AlignedMTL	sgd	0.1	0.6684	0.9103	0.0224	113.11	88.37 ±0.53
Adatask	adam	0.0005	0.7039	0.9196	0.0146	52.17	21.28 ±0.35
MTL-IO	sgd	0.1	0.6957	0.9172	0.0233	110.19	86.46 ±1.63

Table A4: Results for different MTO methods and optimizers on CityScapes [9] using DeepLabV3+ [5]. The best score per metric is highlighted for each MTO method as well as over all methods and optimizers. Adam is Pareto dominant over SGD+mom in a direct pairwise comparison across all MTO methods.

MTO	Optimizer	lr	Sem.Seg.		Depth		DeltaM ↓
			mIoU ↑	pixAcc ↑	AbsErr ↓	RelErr ↓	
STL	adam		0.7203	0.9253	0.0132	47.37	
EW	adam	0.001	0.7247	0.9268	0.0128	47.73	-0.80 ±0.69
EW	signSGD	0.0005	0.7188	0.9249	0.0134	52.47	3.07 ±2.70
EW	sgd	0.05	0.7100	0.9217	0.0174	120.34	46.88 ±2.02
UW	adam	0.001	0.7224	0.9259	0.0122	44.37	-3.65 ±0.61
UW	signSGD	0.001	0.7172	0.9244	0.0127	48.31	-0.35 ±2.23
UW	sgd	0.0005	0.7003	0.9187	0.0171	116.09	44.47 ±1.91
RLW	adam	0.001	0.7230	0.9263	0.0133	47.76	0.26 ±1.08
RLW	signSGD	0.001	0.7185	0.9244	0.0133	54.75	4.09 ±0.39
RLW	sgd	0.05	0.7070	0.9205	0.0176	123.13	48.84 ±1.79
IMTL	adam	0.001	0.7226	0.9259	0.0121	45.25	-3.38 ±0.92
IMTL	signSGD	0.001	0.7177	0.9243	0.0128	49.61	0.57 ±3.75
IMTL	sgd	0.005	0.7027	0.9192	0.0185	122.37	50.33 ±3.30
PCGrad	adam	0.001	0.7247	0.9272	0.0130	47.24	-0.58 ±0.56
PCGrad	signSGD	0.001	0.7187	0.9248	0.0132	53.35	3.28 ±1.41
PCGrad	sgd	0.05	0.7083	0.9212	0.0173	122.52	47.90 ±3.68
CAGrad	adam	0.001	0.7245	0.9264	0.0124	45.56	-2.59 ±0.68
CAGrad	signSGD	0.001	0.7154	0.9243	0.0128	49.06	0.37 ±0.41
CAGrad	sgd	0.1	0.7096	0.9220	0.0172	120.24	46.58 ±2.21
AlignedMTL	adam	0.0005	0.7225	0.9259	0.0122	47.70	-1.79 ±0.70
AlignedMTL	signsgd	0.001	0.7169	0.9241	0.0127	47.56	-0.70 ±0.61
AlignedMTL	sgd	0.1	0.7096	0.9218	0.0174	120.38	46.94 ±1.19
Adatask	adam	0.001	0.7234	0.9260	0.0124	47.21	-1.77 ±0.86
MTL-IO	sgd	0.05	0.7098	0.9217	0.0187	120.61	49.57 ±2.28

Table A5: Results for different MTO methods and optimizers on NYUv2 [39] using SegNet [1]. The best score per metric is highlighted for each MTO method as well as over all methods and optimizers. Using Adam yields in superior performance in the majority of cases, both when considering the individual metrics and the overall Δ_m -metric. We note that Δ_m is more effected by the normal task due to the higher number of corresponding metrics as can be observed in the case of UW.

MTO	Optimizer	lr	Sem.Seg.		Depth		Normal			DeltaM ↓		
			mIoU ↑	pixAcc ↑	AbsErr ↓	RelErr ↓	Mean ↓	Median ↓	11.25 < 22.5 < 30.0 ↑			
STL	adam		0.392	0.646	0.607	0.258	24.74	18.49	0.308	0.582	0.700	
EW	adam	0.0001	0.398	0.650	0.530	0.212	29.53	25.02	0.216	0.454	0.584	10.08 ±2.84
EW	signSGD	0.0001	0.389	0.647	0.543	0.220	30.18	25.93	0.204	0.438	0.569	12.75 ±2.24
EW	sgd	0.01	0.384	0.644	0.551	0.227	30.12	25.72	0.212	0.443	0.571	12.84 ±0.65
UW	adam	0.0001	0.401	0.652	0.522	0.213	27.93	22.80	0.243	0.494	0.623	5.42 ±1.04
UW	signSGD	0.0001	0.384	0.634	0.535	0.218	28.36	23.45	0.233	0.482	0.612	8.05 ±1.18
UW	sgd	0.05	0.383	0.642	0.551	0.218	27.07	21.66	0.259	0.516	0.644	4.46 ±2.13
RLW	adam	0.0001	0.390	0.638	0.537	0.218	30.83	26.78	0.196	0.424	0.554	14.28 ±2.38
RLW	signSGD	0.0001	0.375	0.636	0.544	0.226	29.38	24.77	0.217	0.458	0.589	11.42 ±1.02
RLW	sgd	0.05	0.369	0.633	0.572	0.233	31.21	27.17	0.198	0.420	0.546	16.82 ±1.16
IMTL	adam	0.0001	0.380	0.644	0.524	0.216	26.35	20.77	0.270	0.534	0.660	2.06 ±1.31
IMTL	signSGD	0.0001	0.374	0.639	0.527	0.212	26.26	20.65	0.272	0.537	0.663	1.97 ±0.832
IMTL	sgd	0.05	0.396	0.656	0.532	0.215	26.16	20.38	0.277	0.542	0.666	0.72 ±0.68
PCGrad	adam	0.0001	0.406	0.654	0.529	0.215	28.60	23.75	0.231	0.477	0.606	7.39 ±0.86
PCGrad	signSGD	0.0001	0.394	0.649	0.556	0.219	28.98	24.25	0.223	0.467	0.598	9.59 ±1.02
PCGrad	sgd	0.01	0.389	0.644	0.547	0.223	29.76	25.22	0.214	0.451	0.580	11.61 ±0.36
CAGrad	adam	0.0001	0.405	0.661	0.527	0.211	25.85	20.02	0.282	0.550	0.674	-0.65 ±0.96
CAGrad	signSGD	0.0001	0.393	0.648	0.546	0.217	26.21	20.58	0.272	0.538	0.665	1.67 ±0.61
CAGrad	sgd	0.05	0.400	0.656	0.547	0.223	26.39	20.78	0.268	0.534	0.662	2.06 ±0.65
AlignedMTL	adam	0.0001	0.385	0.648	0.519	0.212	25.51	19.66	0.288	0.557	0.680	-0.86 ±0.14
AlignedMTL	signsgd	0.0001	0.363	0.637	0.528	0.211	25.86	20.02	0.282	0.550	0.674	0.90 ±0.54
AlignedMTL	sgd	0.05	0.371	0.642	0.531	0.214	26.41	20.71	0.272	0.535	0.661	2.33 ±1.00
adatask	adam	0.0001	0.394	0.650	0.518	0.211	26.29	20.67	0.273	0.536	0.661	1.00 ±0.8
MTL-IO	sgd	0.01	0.377	0.637	0.551	0.225	30.05	25.50	0.215	0.447	0.574	12.69 ±1.21

Table A6: Results for different MTO methods and optimizers on NYUv2 [39] using DeepLabV3+ [5]. The best score per metric is highlighted for each MTO method as well as over all methods and optimizers. We note a full dominance of Adam over SGD+mom on both the depth and normal tasks as well as on the Δ_m -metric. Overall, best results for all metrics were also achieved using Adam as optimizer.

MTO	Optimizer	lr	Sem.Seg.		Depth		Normal								
			mIoU \uparrow	pixAcc \uparrow	AbsErr \downarrow	RelErr \downarrow	Mean \downarrow	Median \downarrow	< 11.25 \uparrow	< 22.5 \uparrow	< 30.0 \uparrow	DeltaM \downarrow			
STL	adam		0.552	0.767	0.365	0.152	21.16	14.52	0.402	0.668	0.768				
EW	adam	0.0001	0.552	0.770	0.352	0.143	22.54	16.05	0.366	0.634	0.742	2.70	± 0.12		
EW	signSGD	0.0001	0.554	0.766	0.362	0.147	22.69	16.15	0.364	0.630	0.739	3.60	± 0.38		
EW	sgd	0.01	0.556	0.769	0.365	0.147	23.35	16.76	0.352	0.617	0.727	5.21	± 0.18		
UW	adam	0.0005	0.532	0.755	0.358	0.141	22.01	15.30	0.383	0.650	0.753	1.59	± 0.14		
UW	signSGD	0.0005	0.526	0.748	0.366	0.146	22.18	15.46	0.380	0.645	0.749	2.90	± 0.79		
UW	sgd	0.01	0.557	0.769	0.364	0.148	22.37	15.69	0.374	0.641	0.746	2.57	± 0.56		
RLW	adam	0.0001	0.556	0.768	0.360	0.150	22.37	15.87	0.370	0.638	0.745	2.96	± 0.55		
RLW	signSGD	0.0001	0.557	0.768	0.363	0.146	22.40	15.84	0.371	0.638	0.745	2.74	± 0.30		
RLW	sgd	0.05	0.541	0.762	0.368	0.151	23.00	16.44	0.357	0.625	0.734	5.15	± 0.54		
IMTL	adam	0.0005	0.532	0.756	0.353	0.140	21.34	14.61	0.399	0.666	0.766	-0.39	± 0.05		
IMTL	signSGD	0.0001	0.552	0.767	0.359	0.146	21.81	15.22	0.385	0.652	0.756	1.12	± 0.16		
IMTL	sgd	0.05	0.545	0.762	0.367	0.150	21.63	14.98	0.390	0.658	0.760	1.30	± 0.40		
PCGrad	adam	0.0001	0.558	0.772	0.357	0.146	22.33	15.81	0.371	0.639	0.746	2.34	± 0.48		
PCGrad	signSGD	0.0001	0.553	0.766	0.360	0.148	22.61	16.11	0.365	0.631	0.739	3.55	± 0.13		
PCGrad	sgd	0.01	0.556	0.769	0.361	0.147	23.36	16.79	0.351	0.617	0.728	5.10	± 0.28		
CAGrad	adam	0.0005	0.531	0.755	0.357	0.143	21.42	14.67	0.399	0.664	0.764	0.10	± 0.55		
CAGrad	signSGD	0.0001	0.550	0.766	0.361	0.146	21.94	15.27	0.383	0.650	0.754	1.49	± 0.12		
CAGrad	sgd	0.05	0.556	0.768	0.360	0.144	21.77	14.99	0.391	0.657	0.759	0.42	± 0.07		
AlignedMTL	adam	0.0005	0.531	0.752	0.355	0.144	21.15	14.49	0.403	0.669	0.768	-0.33	± 0.41		
AlignedMTL	signSGD	0.0005	0.527	0.751	0.360	0.144	21.35	14.60	0.400	0.666	0.765	0.25	± 0.21		
AlignedMTL	sgd	0.1	0.550	0.766	0.367	0.150	21.59	14.88	0.393	0.659	0.761	0.95	± 0.62		
adataset	adam	0.0001	0.553	0.768	0.353	0.142	21.44	14.83	0.395	0.661	0.763	-0.39	± 0.21		
MTL-IO	sgd	0.01	0.554	0.768	0.362	0.146	23.31	16.75	0.352	0.617	0.728	5.01	± 0.38		

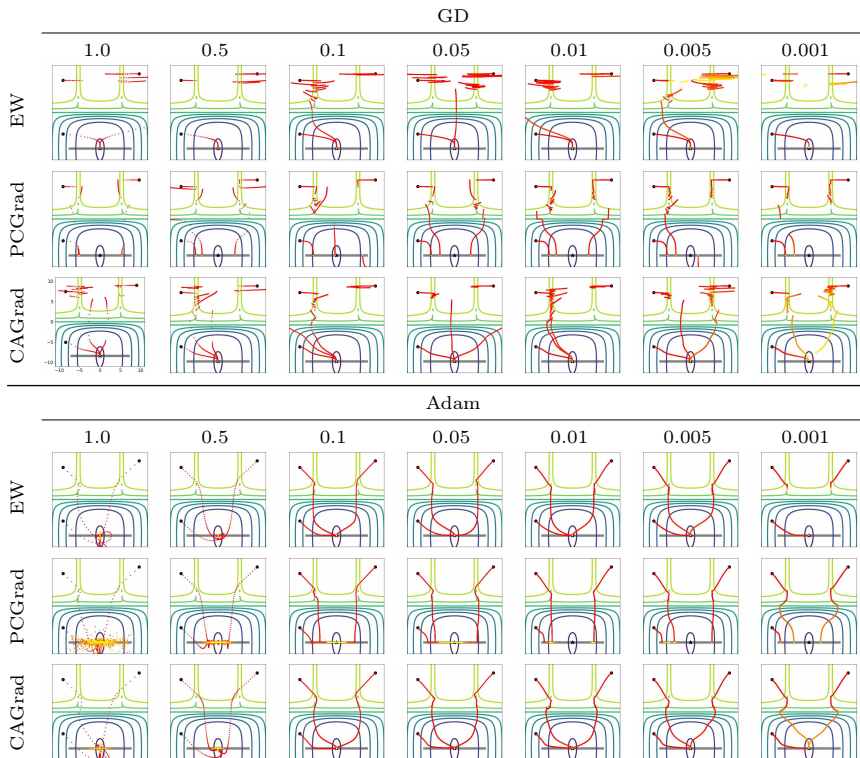


Fig. A5: Extension of Figure 1 with additional learning rates. We show the optimization trajectories for three different seeds (black dots). The Optimization trajectories are colored from red to yellow for 100k iteration steps. The global optimum is depicted as asterisk (*), the Pareto front is highlighted in gray. We note the importance of a good selection of learning rate even for simple toy examples. Moreover, using Adam yields overall faster convergence to the global optimum. We use the original implementation which can be found under <https://github.com/Cranial-XIX/CAGrad>.

Table A7: Number of iterations after which all seeds in toy task experiment from CAGrad [31] have reached the global minimum for different learning rates and optimizer. We show results for additional learning rates compared to the main paper. The maximum iteration number over all three seeds for each MTO method / learning rate / optimizer combination is reported. If not all seeds converged to the global minimum within 100k iteration steps, we denote it as '-'. In several setups, EW+Adam converges fastest to the global minimum. Especially for small learning rates, CAGrad performs advantageous compared to EW. As reported in previous work, we found that PCGrad often would converge only to some point on the Pareto Front. The **best** and *second best* run for each learning rate over all MTO methods are indicated via font type. **Best** and **second best** learning rate + optimizer combination for each MTO are marked via cell background color.

		learning rate								
method		10.0	5.0	1.0	0.5	0.1	0.05	0.01	0.005	0.001*
GD	EW	-	103	-	-	-	-	-	-	-
	PCGrad	-	-	-	-	-	-	-	-	-
	CAGrad	644	-	213	621	8,069	5,732	20,418	34,405	-
Adam	EW	26	<i>37</i>	22	58	709	2,135	9,015	<i>16,005</i>	-
	PCGrad	25	4,960	<i>56</i>	15,741	34,175	41,438	-	-	-
	CAGrad	27	30	<i>32</i>	<i>106</i>	<i>802</i>	<i>7,109</i>	<i>11,239</i>	14,323	57,700

*LR used for results in [31] with Adam

A5 Additional gradient alignment results

We report extended evaluation on gradient similarity in MTL and STL.

Results on CelebA are shown in Fig. A6. Alternatively to a single sample/task, we consider the average gradient in Fig. A7. In Fig. A8, we differentiate between conflicting and supporting gradient pairs when evaluating the cosine similarity. Figure A9 shows the evaluation of the scalar product as an combined measure of similarity in gradient direction and magnitude. We report the number of gradient components which are either positive, negative or zero in Fig. A10. Finally, in Fig. A11, we plot the course of loss functions with respective to the different dataset splits.

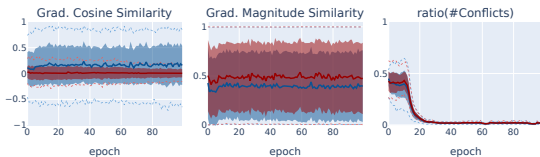


Fig. A6: Gradient similarities and conflicts for CelebA [35]. We report measures with respect to gradient pairs corresponding to either **inter-samples** (fixed task) or **inter-tasks** (fixed sample). We indicate mean (solid line), standard deviation (shaded area), upper (97.5%) and lower (2.5%) percentile (dotted line) over epochs. The gradient alignment is even more similar between different tasks (first column), whereas the magnitude differences are more pronounced in MTL (middle column).

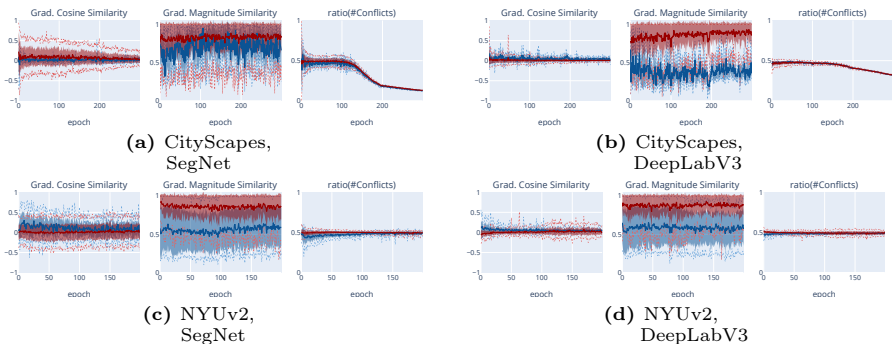


Fig. A7: Gradient similarities when averaging over batch/ losses. In contrast to results shown in Fig. 4, we compute either the average gradient over all tasks when comparing **inter-samples** or the average gradient over all samples within the batch for the comparison between **inter-tasks**. We observed a lower variance in some cases (e.g. CityScapes+Segnet, grad. cosine similarity) which we trace back on noisy gradients being averaged out. Overall, we obtain the same findings as for a direct gradient comparison.

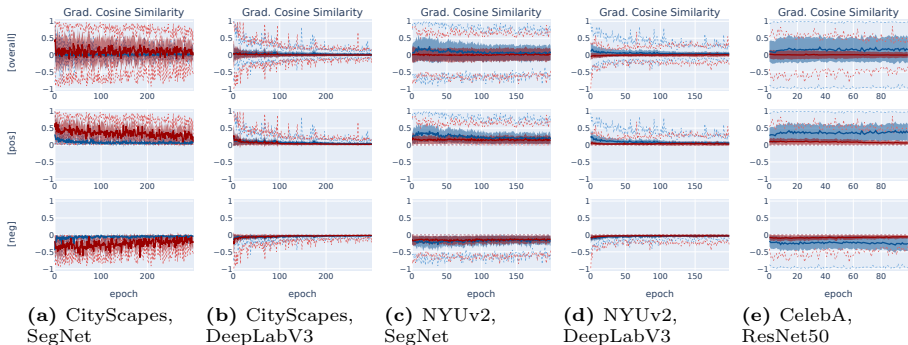


Fig. A8: Differentiation between conflicting and supportive gradients. We report mean (solid line), standard deviation (shaded area), upper (97.5%) and lower (2.5%) percentile (dotted line) of the gradient cosine similarity between either **inter-samples** gradients or **inter-tasks** gradients within an epoch. While showing overall results over all respective gradient pairs (Top) as can be also found in Figure 4, we also show the course of cosine similarity for either gradients that are conflicting ([neg], bottom) or those which have cosine similarity greater than zero ([pos], middle).

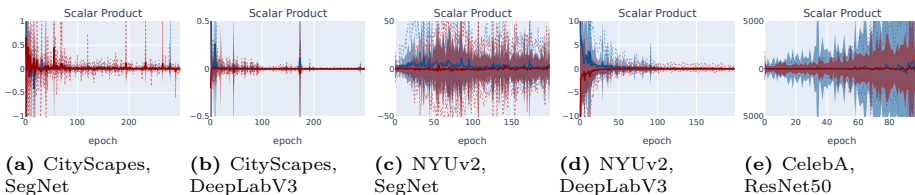


Fig. A9: Scalar product between pairs of gradients. We report mean (solid line), standard deviation (shaded area), upper (97.5%) and lower (2.5%) percentile (dotted line) of the gradient cosine similarity between either gradients of **inter-samples** or **inter-tasks** within an epoch. We observe an overall decrease of the variance of the scalar product for both CityScapes setups and the NYUv2+DeepLabV3 experiment over the training which we explain with evenly smaller overall gradients. Surprisingly, this does not apply for NYUv2 with SegNet or CelebA. Similar to previous results, we do not see any indication for inter-sample gradients being better aligned than inter-tasks gradients.

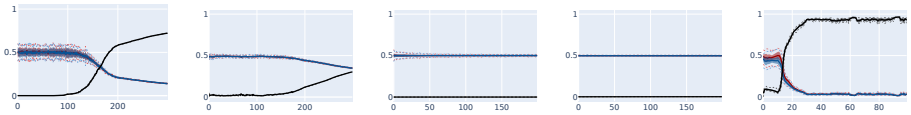
(a) CityScapes,
SegNet(b) CityScapes,
DeepLabV3(c) NYUv2,
SegNet(d) NYUv2,
DeepLabV3(e) CelebA,
ResNet50

Fig. A10: Count of positive/ negative/ zero components in gradients. For each gradient corresponding to one task and one sample, we count the number of **positive** and **negative** as well as **zero-valued** scalar entries. As expected, the amount of positive and negative values is approximately equal during the entire time of training along all experiments. For experiments on CityScapes and CelebA, we found that an increasing number of network components would not receive gradient updates anymore starting at some point in training. This especially holds for CelebA, where we assume to happen because of the ReLU activation functions used in ResNet18.

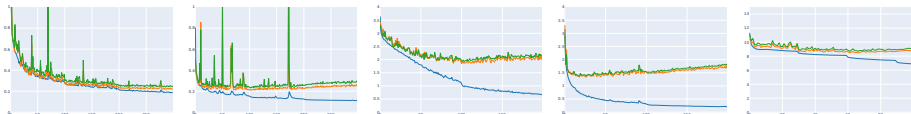
(a) CityScapes,
SegNet(b) CityScapes,
DeepLabV3(c) NYUv2,
SegNet(d) NYUv2,
DeepLabV3(e) CelebA,
ResNet50

Fig. A11: Loss over experiments for gradient similarity experiment. We visualize the loss with respect to the **training**, **validation**, and **test** set during the training process of the gradient similarity experiments.

A6 Additional results for out-of distribution generalization

We present additional results on generalization performance to corrupted data on CityScapes with SegNet as well as on NYUv2 with either choice of network in Fig. A12 and Tabs. A8 and A9. We further show absolute scores for all setups in Tabs. A10 and A11

Table A8: Out-Of Distribution transfer on corrupted CityScapes [9] dataset for different networks and MTO methods. We report difference between relative performance decrease for single-task and multi-task learning averaged over all modes of corruption and all levels of severity (cf. Equation (6)). A value lower than zero indicates a better generalization capability of the MTL backbone, a positive value displays that the STL backbone shows a lower decrease when evaluated on the corrupted data. Results are averaged over runs for three seeds for both multi-task and single-task models. Overall, we observe a slight benefit in performance for the depth task when training for multiple tasks.

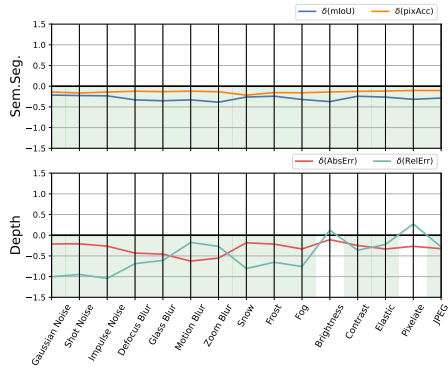
Network	MTO	Sem.Seg.		Depth		Mean
		δ_{mIoU}	δ_{pixAcc}	δ_{AbsErr}	δ_{RelErr}	
SegNet	EW	-0.2922	-0.1386	-0.3175	-0.4949	-0.3108
	UW	0.0854	0.0421	0.7799	-0.2118	0.1739
	RLW	0.0699	0.0307	0.6553	-0.5652	0.0477
	IMTL	0.0696	0.0243	0.5384	0.1108	0.1858
	PCGrad	0.0824	0.0316	0.4106	-0.6392	-0.0286
	CAGrad	0.0561	0.0213	0.3860	-0.3100	0.0383
DeepLabV3	EW	0.0087	0.0017	-0.0108	-0.1826	-0.0457
	UW	0.0110	0.0018	0.1179	0.0861	0.0542
	RLW	0.0263	0.0084	-0.0809	-0.3595	-0.1015
	IMTL	0.0172	0.0041	0.1747	0.0857	0.0704
	PCGrad	0.0090	0.0019	0.0394	-0.2240	-0.0434
	CAGrad	0.0224	0.0067	0.0898	-0.2841	-0.0413

Table A9: Out-Of Distribution transfer on corrupted NYUv2 [39] dataset for different multi-task optimization methods. We report difference between relative performance decrease for single-task and multi-task learning averaged over all modes of corruption and all levels of severity (cf. Equation (6)). A value lower than zero indicates a better generalization capability of the MTL backbone, a positive value displays that the STL backbone shows a lower decrease when evaluated on the corrupted data. Results are averaged over runs for three seeds for both multi-task and single-task models. While for DeepLabV3 largely benefits from MTL, this is not the case for SegNet. Over both networks, EW profits shows lowest relative performance decrease among all MTO methods. Interestingly we found that even for different metrics corresponding to the same task, either the multi-task or single-task learning model would show lower decrease in performance on the corrupted data.

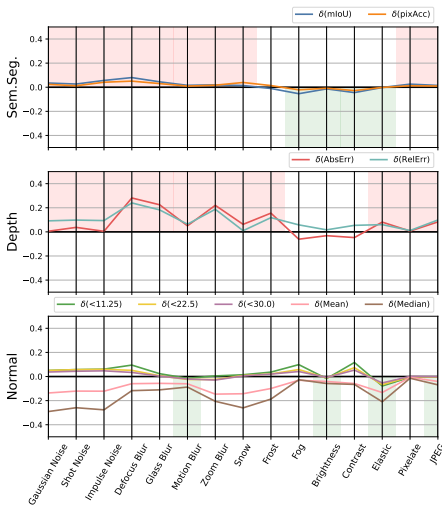
Network	MTO	Sem.Seg.		Depth		Normal				Mean	
		δ_{mIoU}	δ_{pixAcc}	δ_{AbsErr}	δ_{RelErr}	δ_{Mean}	δ_{Median}	$\delta_{<11.25}$	$\delta_{<22.5}$		$\delta_{<30.0}$
SegNet	EW	0.0139	0.0134	0.0715	0.0922	-0.0836	-0.1492	0.0293	0.0168	0.0116	-0.0018
	UW	0.0166	0.0149	0.1146	0.1225	-0.0564	-0.0984	0.0313	0.0207	0.0164	0.0204
	RLW	0.0174	0.0223	-0.0062	0.0281	-0.1048	-0.1857	0.0229	0.0089	0.0055	-0.0213
	IMTL	0.0073	0.0123	0.1108	0.1247	-0.0186	-0.0390	0.0361	0.0274	0.0228	0.0315
	PCGrad	0.0186	0.0174	0.0720	0.0817	-0.0702	-0.1271	0.0264	0.0158	0.0121	0.0052
	CAGrad	0.0061	0.0116	0.1172	0.1428	-0.0082	-0.0202	0.0465	0.0286	0.0223	0.0385
DeepLabV3	EW	-0.0289	-0.0187	-0.1194	-0.1249	-0.1182	-0.1947	-0.0409	-0.0288	-0.0238	-0.0776
	UW	-0.0268	-0.0165	-0.0263	-0.0219	-0.0465	-0.0701	-0.0237	-0.0139	-0.0113	-0.0286
	RLW	-0.0084	-0.0054	-0.0075	-0.0187	-0.0390	-0.0597	-0.0051	0.0009	0.0005	-0.0158
	IMTL	-0.0211	-0.0167	0.0130	0.0059	-0.0153	-0.0219	-0.0072	-0.0045	-0.0038	-0.0079
	PCGrad	-0.0102	-0.0081	-0.0242	-0.0327	-0.0504	-0.0800	-0.0236	-0.0107	-0.0076	-0.0275
	CAGrad	-0.0139	-0.0129	0.0022	-0.0123	-0.0096	-0.0063	0.0023	0.0047	0.0034	-0.0047

Network	MTO	Sem.Seg.		Depth	
		mIoU	pixAcc	AbsErr	RelErr
SegNet	STL	0.3774	0.7241	0.0592	87.06
SegNet	EW	0.3783	0.7399	0.0533	95.17
SegNet	UW	0.3689	0.7273	0.0503	77.86
SegNet	RLW	0.3744	0.7321	0.0526	96.26
SegNet	IMTL	0.3684	0.7363	0.0479	78.92
SegNet	PCGrad	0.3678	0.7310	0.0515	94.44
SegNet	CAGrad	0.3769	0.7397	0.0479	92.75
DeepLabV3	STL	0.5732	0.8593	0.0244	98.97
DeepLabV3	EW	0.5769	0.8619	0.0253	104.37
DeepLabV3	UW	0.5801	0.8632	0.0240	99.67
DeepLabV3	RLW	0.5634	0.8557	0.0270	103.22
DeepLabV3	IMTL	0.5769	0.8617	0.0244	101.26
DeepLabV3	PCGrad	0.5742	0.8609	0.0263	105.46
DeepLabV3	CAGrad	0.5690	0.8576	0.0259	104.90

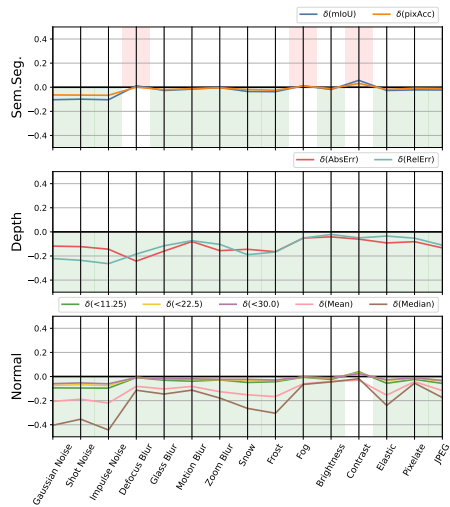
Table A10: Results for evaluating on corrupted CityScapes [9]. Scores are averaged over all corruption modes, level of severity and three seeds.



(a) CityScapes, SegNet



(b) NYUv2, SegNet



(c) NYUv2, DeepLabV3

Fig. A12: Transfer to out-of-distribution data for MTL and STL. For every task and respective metrics, we show the difference over relative performance decrease over all corruption modes averaged over five levels of severity and three runs. EW was used to train the MTL model on uncorrupted data. We color blocks in case either **STL** or **MTL** is able to handle the respective corruption better for all metrics of one task. Regarding the CityScapes dataset, the performance on both task would strongly benefit in MTL setup. A similar behavior can be seen for NYUv2+DeepLabV3. Using SegNet on NYUv2, however, shows preferences towards STL features. Overall, we see a minor indication that MTL result in features that would generalize better to corrupted data.

Network	MTO	Sem.Seg.		Depth		Normal				
		mIoU	pixAcc	AbsErr	RelErr	Mean	Median	< 11.25	< 22.5	< 30.0
SegNet	STL	0.2282	0.4783	0.8389	0.3156	32.05	26.60	0.1994	0.4390	0.5608
SegNet	EW	0.2253	0.4750	0.7702	0.2886	36.06	32.90	0.1306	0.3263	0.4529
SegNet	UW	0.2266	0.4750	0.7847	0.2913	34.90	31.25	0.1445	0.3538	0.4814
SegNet	RLW	0.2182	0.4587	0.7718	0.2957	37.09	34.39	0.1165	0.3045	0.4298
SegNet	IMTL	0.2190	0.4743	0.7804	0.2885	33.89	29.67	0.1609	0.3812	0.5085
SegNet	PCGrad	0.2279	0.4751	0.7790	0.2900	35.34	31.90	0.1388	0.3423	0.4696
SegNet	CAGrad	0.2324	0.4850	0.7822	0.2897	33.50	29.10	0.1648	0.3908	0.5183
DeepLabV3	STL	0.3793	0.6285	0.5342	0.2111	27.32	21.25	0.2853	0.5286	0.6414
DeepLabV3	EW	0.3644	0.6132	0.5594	0.2181	29.88	24.80	0.2359	0.4657	0.5851
DeepLabV3	UW	0.3836	0.6321	0.5137	0.2003	27.75	21.89	0.2738	0.5169	0.6324
DeepLabV3	RLW	0.3861	0.6338	0.5290	0.2081	28.33	23.00	0.2566	0.4964	0.6162
DeepLabV3	IMTL	0.3773	0.6323	0.5208	0.1991	27.27	21.34	0.2830	0.5273	0.6412
DeepLabV3	PCGrad	0.3932	0.6409	0.5168	0.2025	28.05	22.44	0.2659	0.5063	0.6238
DeepLabV3	CAGrad	0.3738	0.6289	0.5266	0.2022	27.68	21.86	0.2754	0.5177	0.6324

Table A11: Results for evaluating on corrupted NYUv2 [39]. Scores are averaged over all corruption modes, level of severity and three seeds.